Alexandru Ioan Cuza
University

Faculty of Physics

Plasma diagnostics by electrical probes

Practicum manual and documentation

L. Sirghi, G. Popa, D. Alexandroaiei, C. Costin

Iaşi, ROMANIA

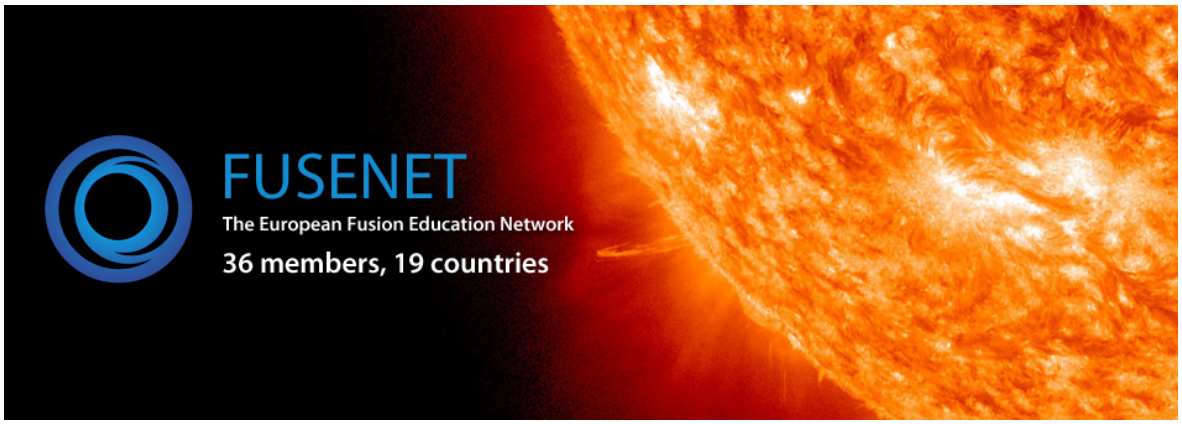

The present manual and documentation has been authored by a group of professors at Faculty of Physics of "Al. I. Cuza" University, Iasi, Romania as a documentation of the FUSENET WP 7 proposal "Plasma diagnostics by electrical probes". The manual is designed to serve as a guide to students and instructors willing to learn and teach, respectively, the basic theoretical and practical principles of plasma diagnostics by electrical probes. The documentation on construction of multipolar confinement plasma device and electrical probes is giving technical details to those who are willing to reproduce the experimental setup and probes used in the present practicum.

Authors

2011, Iasi, Romania

Content

PRACTICUM 0

1. Obtaining of plasma in a multipolar magnetic confinement device and its (plasma) parameters

D. Alexandroaiei

1.1 Introduction

Plasma is a mixture of electrically charged particles (electrons, positive and negative ions) and neutrals which are in free thermal moving. Known as the fourth state of mater, this system is electrically neutral and is governed by the laws of thermodynamics and electromagnetism. Starting from a certain gas, the plasma sources have to provide the charge carriers in sufficient concentration and energy, according to their purposes in the research laboratories or industry. Plasma parameters as ionization degree, temperatures of the charge carriers, plasma quiescence and homogeneity, etc, are important for various applications. Not less important for a plasma source, it is its cost and easiness of machination.

Being known as the fourth state of mater, a plasma can be produced by a substantial heating of a gas, which at high temperature is transformed in plasma ($k_BT \sim eV_i$, k_B – the Boltzmann constant, V_i – the ionization potential of the gas neutrals). Unfortunately, this way of producing plasma spends too much energy and is not in general use. For this reason the most used way to make gaseous plasmas is to "energize" the few free electrons existent in every gas (as result of the telluric radioactivity or the action of the cosmic radiation) to produce ionization of the gas neutrals ($mv^2/2 > eV_i$). This is produced using an electric field E by applying a voltage V between two electrodes (cathode and anode) a electric current source ($E = V/d$, d – the distance between the two electrodes) for acceleration of the free electrons. The electrons and ions which result as ionization products are accelerated in the same applied electric field and they can produce new ionization processes.

The electron-atom collisions and the ionization process are treated statistically. Let α to be the first Townsend coefficient as the probability that an electron moving from cathode, in the inter-electrode space, ionizes an atom on a distance of 1 cm. Considering all electrons (resulted from the first one leaving the cathode) produced in all consecutive ionization processes along cathode-anode distance, their number is increasing exponentially with the distance, d, as $\exp(\alpha d)$ [1-3].

On the other hand, the same number $\exp(\alpha d)$ of ions produced in ionizations move towards cathode. Here, they strike the cathode surface, and produce emission of other electrons through γ secondary Townsend processes. If γ is the number of electrons emitted at

cathode for one bombarding ion, the discharge electric current I (in general very small) through the source circuit is [1-3]:

$$I = I_0 \cdot \exp(\alpha \cdot d) / \{1 - \gamma \cdot [\exp(\alpha \cdot d) - 1]\}, \qquad (1.1)$$

where I_0 is the current of the primary electrons assured by external conditions as cathode photo or thermo electronic emission, etc…

It is clear that if each primary electron leaving cathode is compensated with another one by its primary α (volume) and secondary γ (cathode surface) processes, namely:

$$1 = \gamma \cdot [\exp(\alpha \cdot d) - 1], \qquad (1.2)$$

(see the denominator of (1) if $I \rightarrow \infty$), there are conditions of self-sustaining, and the discharge, respectively the plasma source is now an *autonomous* one, arising conditions for an usual glow discharge or even those for the arc discharge if the cathode material permits. Now, the current I depends no more on I_0 , its value being controlled by the electrical power supply and the external resistor R_S from the plasma source circuit. These discharges are stabile if $R_S > R_d$ where $R_d = (\delta V/\delta I)$ is the internal differential resistance of the discharge [1.1-1.3].

Different parts of the glow discharge are used according their applications. For example, short discharges with only the negative glow are frequently used in applications as surface cleaning and thin film depositions. Different discharge regimes (relative to the voltage–current characteristics) of the glow discharge, normal, abnormal, or arc are used for different applications.

The gas pressure p is the parameter that affects drastically the elementary processes in the plasma discharge. The mean free path for the electron-neutral ionizing collisions, λ_i ($\lambda_i \sim 1/ p$), should be sufficient of long, but no longer than d, for the electrons to gain the ionization energy from the applied electric field. In this way the existence of sufficient numbers of ionization processes is assured in order to satisfy the equation (2). For a given pressure p and inter-electrode distance d, this is happening at a discharge voltage V_B named the *breakdown voltage,* which is:

$$V_B = B \cdot (pd) / [\ln(pd) + A], \qquad (1.3)$$

where A and B are constants that depends on the physical properties of the cathode and discharge gas. This dependence of V_B *on* $(p \cdot d)$ is called the *Paschen law*, and it divides the $(V,(p \cdot d))$ plane, breakdown voltage - product pressure*electrode spacing, in two regions – the upper one without discharge and the lower one with glow discharge, and, what is very important, this equation, has a minimum, the *Paschen minimum,* $V_{B\ min} = V_B\ (p \cdot d)_0$, that means for a gas and cathode material pair there exists a minimum voltage of breakdown for a

given product $(p \cdot d)_0$ [1.1-1.3]. Another important fact is that the breakdown voltage can be reduced using special configurations of electrodes as in the *double cathode effect* or using an uniform magnetic field (acting on the trajectory of the primary electrons) which both increase the ionizing efficiency through "growing" the effective electrode spacing.

Practically, for any plasma source the voltage, discharge current intensity, electrode configuration (with an equivalent inter-electrode distance and the material of cathode), the gas pressure, and the working gas are the most important given constructive parameters. For low pressures cases (10^{-5} - 10^{-4} Torr), when $\lambda i > d$, the primary electrons arrives to anode making very few or no ionizing processes. In this case the discharge current is very low. For this reason, to achieve the breakdown and high density plasma the discharge is maintained in the *non-autonomous regime*. This discharge may use cathodes heated at thermoemission, made as a multi-filament uniformly distributed inside or around the discharge volume [1.4]. The filaments generate electron beams by thermo-electron emission and if the pressure is very low their current is limited at a maximal value given by the Richardson-Dushman law:

$$I = R \cdot A \cdot T^2 \cdot \exp(-W_f/kT) \qquad (1.4)$$

where R is the Richardson constant, A is the filament active surface, T is the temperature, and W_f the work function of the filament surface. However, this discharge with hot cathode works at medium pressures (~1 Torr) gas as the old gaseous diodes or the thyratrones. In direct conduction they work at low voltage and high current intensity, similar to the arc discharge.

Another kind of plasma sources uses so called a *synthesized plasma* [5], when besides the filament-cathode, which emits electrons, the anode acts as source of ions through thermo-ionic emission.

1.2 Multipolar magnetic confinement discharges

With the goal to obtain a homogeneous and relatively dense plasma in a large volume at low gas pressure (at $\lambda_i > d$ or $\lambda_i \sim d$) we use a non-autonomous discharge with hot cathode (filament) and multipolar magnetic confinement of electrons at the anode in order to increase the ionizing efficiency. The probability of the ions resulted in electron ionizing processes to be collected by the cathode (filament) is very low because the filament has a very small surface. In such a way the ions diffuse and remain around centre of the device forming a so-called *diffusion plasma*. The quasi-neutrality condition of plasma is maintained because the space charge of the ions attracts an equal negative space charge of slow electrons (secondary electrons resulted in ionization processes) [1.4]

The intensity of the discharge current, I_d, in this plasma source is maximally limited by the functionality of the double space charge formed between the hot filaments and the

surrounding plasma. Combining the Langmuir condition for plasma double layer [2, 6] and the Bohm criterion [6] from the formation of space charge sheaths results in the fallowing expression of I_d:

$$I_d = \beta \cdot A \cdot e n_0 \cdot (k \cdot T_e / m_i)^{0.5}, \qquad (1.5)$$

where subscripts e and i refer to electrons and ions and the constant β is a parameter closed to unity depending by plasma parameters (n_0, T_e).

Without magnetic confinement the above described plasma source would be very inefficient because it should use many heated filaments (or a single long filament), great electric power to heat them and other resources for device cooling. This inconvenient arises from the fact that the primary electrons arrive directly to the anode without or with few ionizing process. The few secondary electrons are easily collected by the anode and the concentration of the diffusion plasma is of very low density. Therefore, the source uses a special magnetic confinement of the primary electrons in a region situated in vicinity of the anode. In this way the primary electrons are able to produce an increased number of ionizing processes before they are collected by the anode. The secondary electrons are trapped also and the plasma density is increased (without increasing the number of filaments) because the losses of charge carriers are decreased.

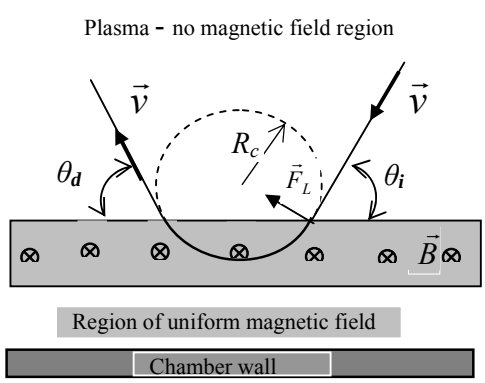

Fig.1.1 Trajectory of an electric charged particle coming into and coming out a region of uniform magnetic field

The basic idea of such of magnetic trap is to create around the plasma a region with uniform magnetic field parallel to the chamber wall. When a charged particle coming from plasma enters in the magnetic region, it is deflected back into the plasma (with an angle, θ_d , equal with the angle of incidence, θ_i, as in a optical reflection -see Fig. 1.1) due to the action of the Lorentz force, $\vec{F}_L = q(\vec{v} \times \vec{B})$.

Having in mind the value of the cyclotron radius, $R_c = mv/qB$ of the charge-particle trajectory, it results that the penetration distance into the B field region has a maximal value of $2 \cdot R_c$. The same value is for the distance between the coming into and coming out points of the trajectory relative to magnetic field region (see Fig. 1). For good results these distances have to be very small, fact which is realized by using strong magnetic field so that the charged particles moving through it are collected by the anode. The above considerations

refer specially to the primary electrons because they have greater velocities then the secondary ones.

1.3 General working details of the multipolar magnetic plasma confinement device

In practice, such a magnetic trap is realized using permanent magnets to obtain near the anode wall a multi-line-cusp configuration aligned parallel to the cylindrical plasma chamber. To obtain a cusp configuration, equally distanced row-lines of magnets (with the same polarity) alternate in polarity (Fig 1.2). As it was shown before, and from the general theory of the motion of the electric charged particle in magnetic-cusp traps [1.7], the primary electrons moving towards the anode are reflected back inside the chamber with effect of increasing of their path through the discharge chamber. The secondary electrons are confined by the magnetic cusp trap even better than the primary electrons because they have low kinetic energy. The only particles that are loosed from the trap are those which move normally to the middle of the magnets or are not reflected back at the end of the cusp-mirror magnets [6,7]. These charged particles which traverse the cusp traps near the anode wall determine the discharge current of the plasma source. There is an optimal number of row-lines on chamber inner surface that is depending on magnets and the dimensions of plasma chamber. This is because the increase of the number of lines of magnets does increase the magnetic field intensity, but in the same time increases the effective area of electron loss. Figure 1.2b shows regions with or without plasma (see the space between the magnets, near the anode-wall).

As a fact which illustrates the trapping effect in this kind of plasma source in Fig 1.4 a it is illustrated a comparison of the decays of the plasma in a source with (upper curve) and without (lower curve) magnetic trap, after the bias voltage and the filament heating were turned off [1.7]. The effective time of maintaining of the plasma in the multipolar magnetic source is evidently longer than without magnetic trapping. In Fig 3b the radial dependence of the relative plasma concentrations is presented for three values of the gas pressure. It is observed a good homogeneity but, this is decreasing with the increasing of the gas pressure

Currently, due to their performances, the multipolar magnetic confinement plasma devices have a large variety of applications starting with the basic ones in fundamental research of plasma physics, together with their variants as double or triple plasma machines and as sources of ion or neutral beams [1.8].

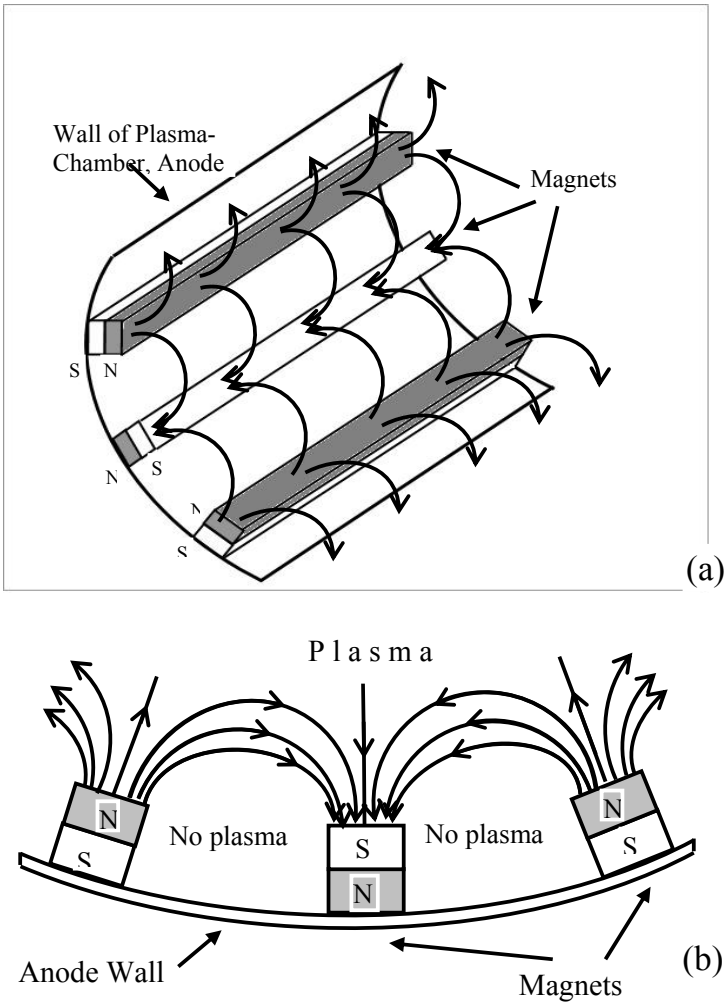

Fig.1.2. (a),(b)-Magnetic field configuration with the positions of the magnets in a multipole cusp plasma source ilustrating the regons with and without plasma trapping

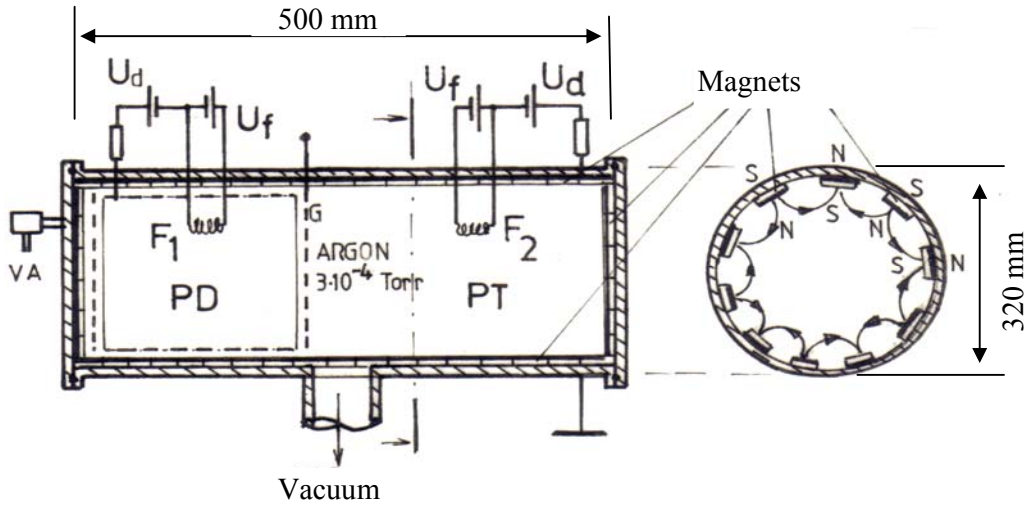

Fig.1.3. Scheme of the multipolar plasma machine from the Plasma Physics Lab of the „Al.I.Cuza" University, Iasi, Romania: PD- driver plasma chamber, PT - target plasma chamber, G – separation grid; F_1, F_2 – filaments, U_d, U_f – power supplies, VA – needle valve for gas pressure setting [1.10].

Typical main plasma parameters for these plasma sources are summarized bellows, [5]:

Electron temperature (T_e)……1 - 5 eV

Ion temperature (T_i).....~0.3 eV

Electron concentration (n_e)…….....10^9-10^{10} cm^{-3}

Ionization degree (n_e/n_n)…… 10^{-3} - 10^{-2}

Quiescence ($\delta n_e/n_e$) ……10^{-3}

Cost/Complexity (in a 1-5 scale)……...2

Specific characteristic: enriched electron tail of EEDF

These devices work very well also as high frequency discharges [8].

1.4 The multipolar magnetic plasma confinement device from Plasma Physics Lab of "Al.I.Cuza" University, Iasi, Romania

The multipolar plasma source from "Al.I.Cuza" University is a double plasma device which allows a large variety of general plasma experiments (ion acoustic plasma wave) and many electric methods of plasma diagnostics [9,10].The device contains two plasma chambers which are galvanic separated, the driver plasma (PD) and the target plasma (PT), each of them with its filament, and can be electrically biased one against the other. The basic vacuum in the two plasma chambers can now attain a value of 10^{-4} mBar after 1 hour of pumping with primary dry and turbo-molecular vacuum pumps. The working gas (argon) is fed into the discharge chamber through a needle-valve at constant flow speed, of which value controls the gas pressure (between 10^{-4} and 10^{-3} mBar).

The constructive details are shown in Fig. 1.3. The two chambers, of cylindrical form, are surrounded by 16 in-line-columns of permanent magnets (in our case made of ferrite – B_{max} ~ 0.3 T). The distance between the row-lines of magnets is about 3 cm. The cylindrical device is ended by flanges through which are the passages for diagnostic probes or other electrods, observation windows, etc…

The filaments are made of wolfram or tantalum wire (0.5mm thickness and 6-9 cm length) and are heated by direct current (intensity about 5A) with the two power supplies U_f. After stabilization of the working gas pressure and the filaments have arrived the regime of thermo-electron emission the discharge is obtained by applying the voltage between the filaments as cathodes and the chamber walls as common anode with the power supplies U_d. A value of U_d around 100 V is sufficient for plasma ignition. Values of 100-300 mA for

discharge current intensity assures relatively homogeneous plasma (see Fig 1.4) with concentration values between 10^9 and 10^{10} cm^{-3}

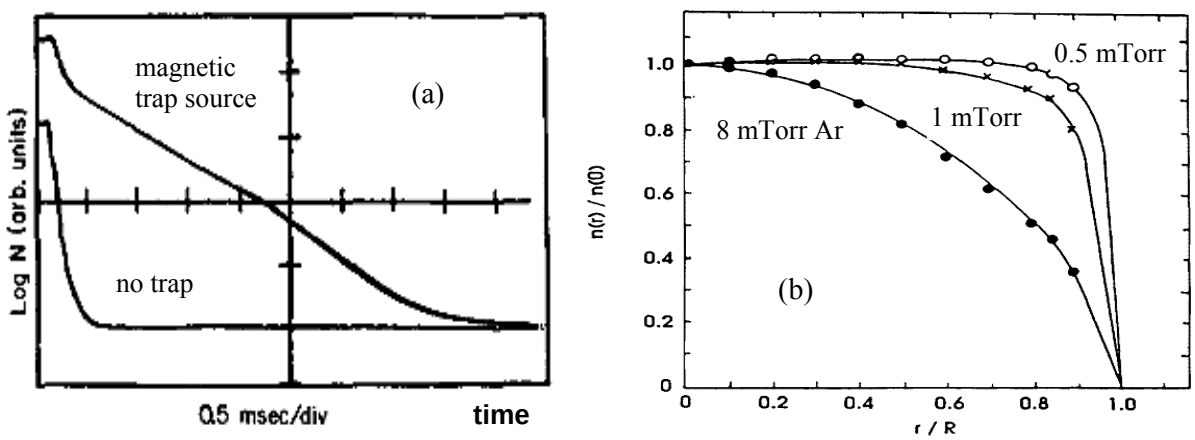

Fig.1. 4 (a) The temporal evolution of the logarithm of plasma concentration during of its decay for the cases with or without a magnetic trap [1.7]. (b) Relative plasma concentration, $n(r)/n(0)$, versus the relative radial position, r/R, in a cylindrical plasma machine for three values of the gas pressure [1.8].

References

[1] Y. Raizer, J. Allen, V. Kisin, *Gas Discharge Physics,* Springer-Verlag, Berlin, Heidelberg, (1991)

[2] M.A. Lieberman and A.J Lichtenberg, *Principles of Plasma Discharges and Materials Processing*, John Wiley, New York, (1994).

[3] S.C. Brown, *Introduction to Electrical Discharges in Gases*, John Wiley, NY, 1966.

[4] R.I.Taylor, K.R. MacKenzie and H. Ikezi, Rev. Sci. Instr., **43,** 1679 (1972)

[5] R. Jones, Physics reports, **61,** 5, 295 (1980)

[6] F.F. Chen *Introduction to Plasma Physics*, Plenum Press, NY, (1974)

[7] I.R. Limpaecher and K. R. MacKenzie, Rev. Sci. Instrum, **44**, 726 (1973).

[8] O.A. Popov, *High density plasma sources,* Noyes Publications, Park Ridge, New Jersey, U.S.A (1995).

[9] G.Popa, L.Sirghi *Basic of Plasma Physics*, Ed. "Al.I.Cuza" University Press, Iasi, Romania, (2000) (in romanian)

[10] G.Popa, D.Alexandroaei, *Guide of Practical Work for PlasmaPhysics* Ed. "Al.I.Cuza" University Press, Iasi, Romania, (1991), (in romanian)

PRACTICUM 1

Determination of temperature and density of the two-Maxwellian electron groups in multi polar magnetically confined plasma by a single Langmuir probe

L. Sirghi

Introduction

Langmuir probes are planar, cylindrical or spherical electrodes inserted into the plasma with the goal of monitoring or measuring various plasma parameters, *i. e.* plasma diagnostics [2.1, 2.2]. Although, Langmuir probe diagnostics is simple in principle, in practice there are many aspects that can affect very much the measurements. For example, all probe diagnostics methods assume that the probe surface is cleaned and it perfectly adsorbs, without chemical reactions, the electrically charged particles collected by it. In practice, the probe surface can be covered by various contaminants, including insulated hydrocarbon molecules from vacuum oil (in case of a vacuum system that uses vacuum oil), or metal oxides. This can affect very much the current collected from plasma by the biased probe. Therefore, before measurements a cleaning of the probe surface by positive ion or electron bombardment is obligatory. There are some other practical complications as it fallows:

1) the plasma is not stable during measurements (the plasma potential, as well as the density, can fluctuate or drift during the time of the probe measurements);

2) the probe draws large currents from plasma, which perturbs the initial state of the plasma and lead to erroneous measurements;

3) distortion of the probe current-voltage characteristics due to bad probe electrical biasing circuitry;

4) elastic, excitation and ionization collisions in the probe sheath (in high pressure plasmas at large values of the probe biasing potential);

5) presence of negative ions;

6) chemical reactions at probe surface;

7) complex I-V characteristics due to non Maxwellian distributions of charged particles (presence of ion or electron beams, etc).

In spite of so many complications, the Langmuir probe diagnostics is widely used because it is relatively simple to use, cheap, and gives reliable values of important plasma

parameters as plasma potential, density and electron temperature. Moreover, in some conditions the single Langmuir probe measurements can provide valuable information on the electron energy distribution function. This plasma laboratory practicum is dedicated to processing of Langmuir probe data acquired in plasma with two Maxwellian populations of electrons, as is the diffusion plasma generated by the *dc* discharge in multi polar magnetically confined plasma device described in the practicum number 1. An analysis of probe I-V probe characteristics without taking into account the presence of the two electron groups in this plasma, *i. e.* a non Maxellian electron energy distribution function, lead to an incomplete or false description of the plasma parameters (electron temperature and density). On the other hand, the analysis of I-V probe characteristics in this case offers a good example of application of an iteration algorithm to extract the values of electron density and temperature for the two groups of electrons in this particular plasma device.

Theory

The most simple probe theory used in processing the probe current-voltage characteristics assumes that the probe current corresponds to collection of charged particles drown from an infinite (the plasma volume is much larger than the probe volume) and simple (formed by neutral atoms, positively ionized atoms, and electrons) plasma. The electron and ion velocity distribution function are considered Maxwellian and the ion temperature, T_i, may be different of electron temperature, T_e (in cold plasmas $T_i << T_e$ while in thermal plasmas, $T_i = T_e$). In these conditions, the probe biasing potential, V_b, the probe geometry, and the plasma parameters are the only factors that determine the value of probe current intensity. Thus, the probe current-voltage characteristic, which is the probe current intensity, I, acquired as a function of probe biasing potential, V_b, has typically three regions, as it is depicted in Fig. 1. The tree regions are:

1) ion saturation region, when $V_b << V_p$ (V_p is the plasma potential) and the probe collects all positive ions in their thermal moving towards probe surface and reject almost all the electrons (V_p-$V_b >> kT_e/e$);

2) electron saturation region, when $V_b > V_p$ and the probe collects all the electrons in their thermal moving towards the probe surface and reject all the positive ions.

3) transient region, when $V_b < V_p$ and the probe rejects partially the plasma electrons. This region contains the information on the plasma electron temperature and electron energy distribution function [2.3].

Conventionally, the current intensity given by electrons collected by the probe, I_e, is considered positive, while the current intensity given by the positive ions collected by the probe, I_i, is considered negative. Thus,

$$I(V_b) = I_e(V_b) - I_i(V_b), \tag{1}$$

where absolute values of I_e and I_i are taken. As it is illustrated in Fig. 2, at $V_b = V_p$, there is no sheath of space charge between the plasma and the probe surface. Therefore, the probe surface at plasma potential collects all the electrons and ions which in their thermal movement come on the probe surface. The thermal current intensity of electrons collected by probe is:

$$I_{e0} = S \cdot e \cdot \int_0^\infty f_{ex}(\mathrm{v}_x)\mathrm{v}_{ex} d\mathrm{v}_{ex} = S \cdot \frac{1}{4} e \cdot n_e < \mathrm{v}_e > = e \cdot n_e \cdot S \cdot \sqrt{\frac{k_B T_e}{2\pi m_e}}, \tag{2}$$

where S is the electron collecting area of the probe, f_{ex}, the electron velocity distribution function along the direction x (perpenducular on the probe surface), e, the elementary electric charge, and m_e, the electron mass.

Similarily, for ions:

$$I_{i0} = S \cdot e \cdot \int_0^\infty f_{ix}(\mathrm{v}_x)\mathrm{v}_{ix} d\mathrm{v}_{ix} = S \cdot \frac{1}{4} e \cdot n_i \cdot < \mathrm{v}_i > = e \cdot n_i \cdot S \cdot \sqrt{\frac{k_B T_i}{2\pi m_i}}, \tag{3}$$

Generally, since $m_i >> m_e$, $<\mathrm{v}_e> >> <\mathrm{v}_i>$ and $I_{i0} << I_{e0}$. For cold plasmas, the ions are heated in a presheath and they comes towards the probe surface with Bohm velocity[2.4], $< \mathrm{v}_{ix} > = \mathrm{v}_B = \sqrt{\frac{k_B T_e}{m_i}}$. Therefore, for cold plasmas the Eq. (3) is written as:

$$I_{i0} = S \cdot e \cdot n_i \cdot \mathrm{v}_\mathrm{B} = e \cdot n_i \cdot S \sqrt{\frac{k_B T_e}{m_i}}. \tag{4}$$

In the region of ion saturation, $I = -I_{i0}$, while in the region of electron saturation $I = I_{e0}$. In these regions a positive, respectively, negative space charge sheath forms between the plasma and the probe surface (Fig. 2). If the sheath thickness is much smaller than the probe dimension, the charge collection surface hase approximately the same area as the active surface of the probe. The most interesting part of the probe *I-V* characteristic is the transient region, when between the probe surface and plasma there is a positive charge sheath that rejects partially the electrons coming from plasma (Fig. 2 B). In this region the electron current has an exponential dependence on V_b. Indeed, in this region V_b is negative with respect to the plasma potential, V_p, and the probe collects all the positive ions entering in the probe sheath and the only electrons that are fast enough to reach the probe surface [electrons

of which kinetic energy, $m\mathrm{v}_x^2/2$, is larger than the mechanical work of the electron retarding electric filed of the probe sheath, $e(V_p\text{-}V_b)$].

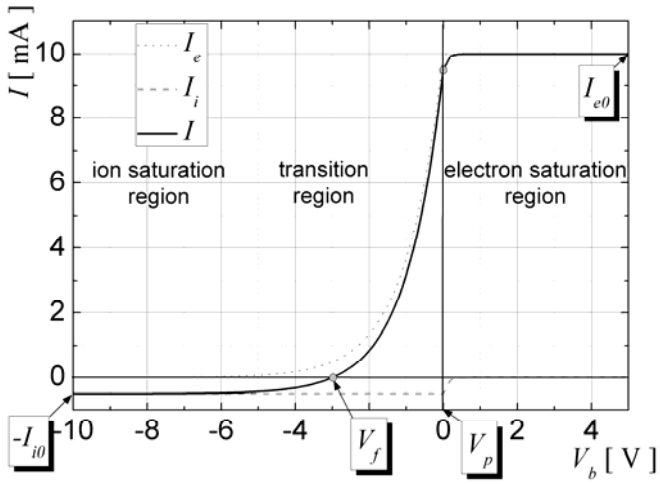

Fig. 1 Theoretical probe I-V characteristic for a plasma with T_e = 1 eV and T_i = 0.1 eV. Values I_{e0} = 10 mA, I_{i0} = 0.5 mA, V_p = 0V and V_f = -3 V are assumed.

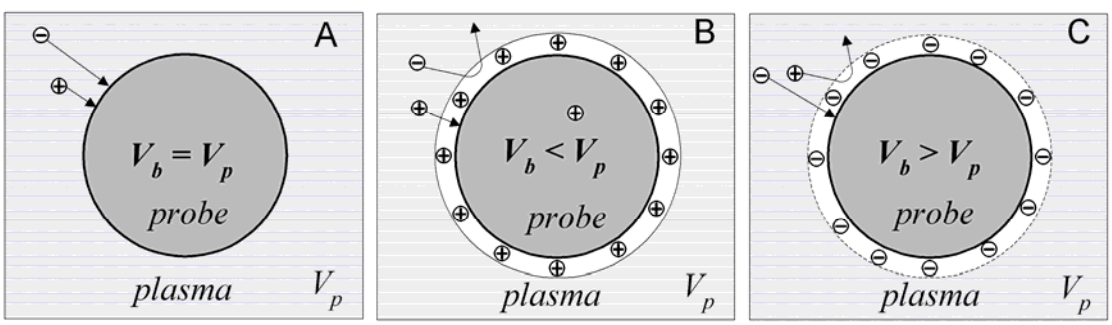

Fig. 2 Collection of charged particles from plasma by a probe biased at plasma potential (A), negatively with respect to plasma potential (B), and positively with respect to plasma potential.

$$I_e(V_b) = S \cdot e \cdot \int_{\mathrm{v}\,\min}^{\infty} f_{ex}(\mathrm{v}_{ex})\mathrm{v}_{ex} d\mathrm{v}_{ex} = I_{0e} \cdot \exp\left(eV_b / k_B T_e\right), \tag{5}$$

where $\mathrm{v}_{\min} = (-2eV_b/m_e)^{1/2}$, V_p = 0, and V_b < 0. This exponential dependence can be used to determine the electron temperature. Thus, the semilogatithmic plot of V-I characteristic in this region is linear and the slope, $tg(\alpha)$, of the linear dependence of $\ln(I_e)$ on V_b is:

$$tg(\alpha) = \frac{\ln(I_{e2}) - \ln(I_{e1})}{V_{b2} - V_{b1}} = \frac{e}{k_B T_e}, \quad (6)$$

where V_{b1} abd V_{b2} are two values of V_b at which the electron current intensity has the values, I_{e1}, respectively, I_{e2}. This computes the electron temperature as:

$$k_B T_e(eV) = \frac{V_{b2} - V_{b1}}{\ln(I_{e2}) - \ln(I_{e1})}. \quad (7)$$

The value of the electron temperature can be used in the Eq (2) of the electron saturation current to compute the electron density:

$$n_e = \frac{I_{e0}}{eS} \cdot \sqrt{\frac{2\pi m_e}{k_B T_e}} \quad (8)$$

It is worthwile to note the value of the probe floating potential, V_f, on the probe I-V characteristic (Fig. 1). This is the probe biasing potential at which the probe current intensity is null, which means that the probe surface at this biasing potential collects equal amounts of electrons and ions:

$$I_e(V_f) = I_i(V_f) \quad (9)$$

Using the expressions $I_i(V_f) = I_{i0}$ and $I_e(V_f) = I_{e0} \cdot exp(V_f/k_B T_e)$,in the Eq. (9) computes the value of V_f as:

$$V_f = k_B T_e \cdot \ln\left(I_{i0}/I_{e0}\right) \quad (10)$$

The probe theory described above works well in plasmas with a single population of Maxwellian electrons, *i. e.* the velocity distribution function of electrons is the Maxwell distribution function at thermodynamic equilibrium temperature T_e. However, the electron velocity distribution function in real plasmas is rarely Maxwellian. Particularly, the diffusion plasma obtained in multipolar magnetically confined plasma device has two Maxwellian electron populations [2.5]. They are *the primary electrons*, which are emitted by cathode, accelerated in the cathode sheath and thermalized due to their excitation and ionization collisions with neutral atoms in the confining magnetic filed region, and *the secondary electrons*, which are the electron resulting from ionization of the neutral atoms. The primary electron group is less numerous than the secondary one ($n_p << n_s$) but more energetic ($T_p > T_s$). The electron energy distribution for this plasma can be written as:

$$f_e(\mathrm{v}) = n_p\left(m_e/2\pi k_B T_p\right)^{3/2} \cdot \exp\left(-m_e \mathrm{v}^2/2k_B T_p\right) + n_s\left(m_e/2\pi k_B T_s\right)^{3/2} \cdot \exp\left(-m_e \mathrm{v}^2/2k_B T_s\right), \quad (11)$$

where n_p, n_s, T_p, and T_s are the densities and, respectively, temperatures of the primary and secondary electron groups. In this case, the electronic probe current in the transient region is the sum of primary and secondary electron current intensities [2.6, 2.7]:

$$I_e(V_b) = S \cdot e \cdot \int_{v\min}^{\infty} f_e(v_{ex}) v_{ex} dv_{ex} = I_{0p} \cdot \exp\left(eV_b / k_B T_p\right) + I_{0s} \cdot \exp\left(eV_b / k_B T_s\right), \quad (12)$$

where I_{0s} and I_{0p} are the electron saturation current intensities corresponding to the two group of electrons and $V_p = 0$. The saturation electron current intensity are computed by:

$$I_{0p} = = e \cdot n_p \cdot S \cdot \sqrt{\frac{k_B T_p}{2\pi m_e}} \quad (13a)$$

$$I_{0s} = = e \cdot n_p \cdot S \cdot \sqrt{\frac{k_B T_s}{2\pi m_e}} \quad (13b)$$

Experiment

Figure 3 presents a probe I-V characteristic acquired for a cylindrical Langmuir probe (tungsten wire with 0.3 mm in diameter and 5 mm in length) in the multipolar magnetically confined plasma obtained by electrical discharge (discharge current intensity of 100 mA, and discharge voltage of 70 V) in air at pressure of 10^{-4} Torr. The multipolar magnetically confined plasma device, the data acquisition system of the probe I-V characteristics and the digital data processing software are described in Annexes. The probe current and biasing voltage data are stored in a file (CSV type) and processed by a specialized homemade software in LabView.

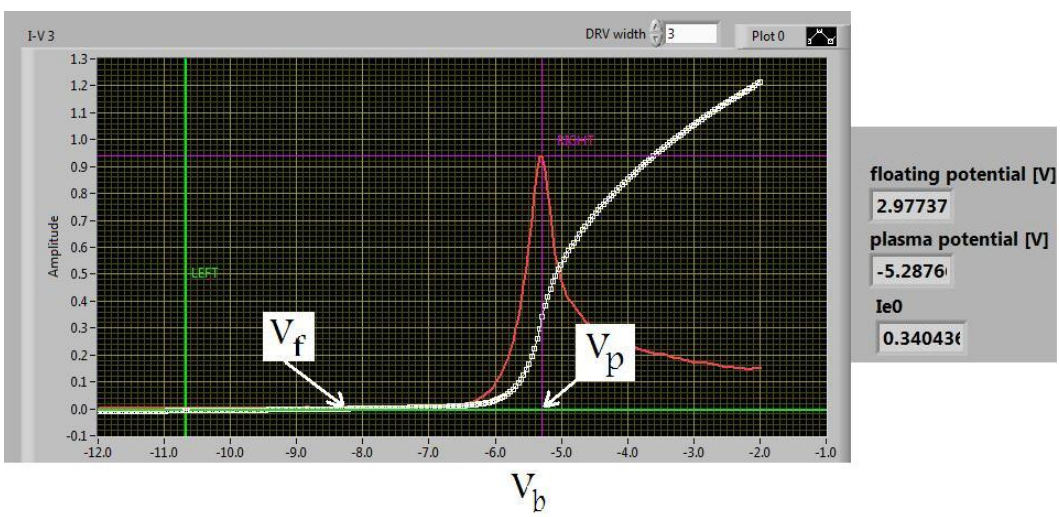

Fig. 3. Plots of $I(V_b)$ probe characteristic (white) and its first derivative (red) used to determine the values of V_p and V_f.

First step in data analysis consists in identifying of the values of plasma potential, V_p, and floating potential, V_f . The plasma potential is identified at the inflexion point on the probe I-V characteristic, which is the position of maximum of the first derivative of $I(V_b)$. On

the plots in Figure 3 is an example of completion of this step in LabView. The values of V_p and V_f -V_p are determined. Note that for $V_b > V_p$ the electronic current does not reach saturation and the probe current intensity continues to increase with the increase of V_b. The cause of this phenomenon will be explained and studied in another practicum. However, the phenomenon makes difficult the identification of V_p and the electron saturation current intensity, I_{e0}, on the I-V probe characteristic. This is why, this data analysis step uses the inflexion point method to determine V_p.

Next step in the data analysis consists in extraction of the electron current from the total probe current. This is done by identifying of the ion saturation current intensity, $-I_{i0}$, (as minimum negative value of the probe current intensity) and approximating I_e with $I+I_{i0}$.

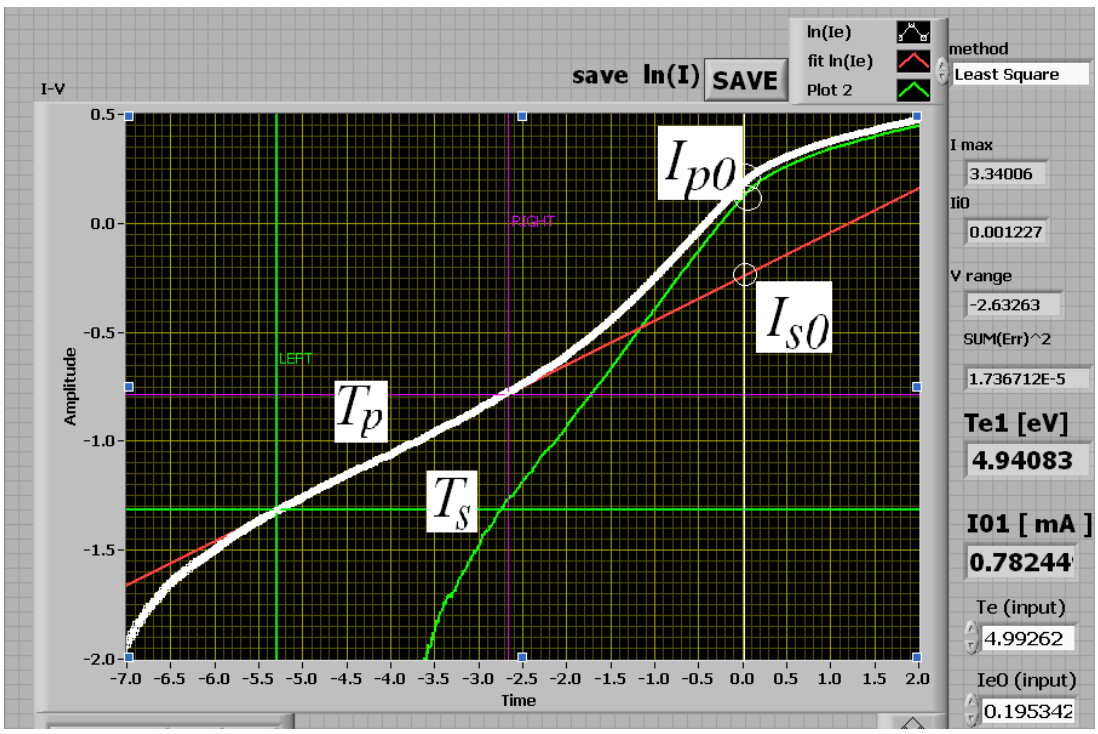

Fig. 4. Example of semi logarithmic plot of $I_e(V_b)$ and separation of the contributions of the secondary (T_s and I_{s0}) and primary (T_p and I_{p0}) electron populations.

Then, the dependence $\ln[I_e(V_b)]$, where V_b is taken with respect of the value of V_p found in the first step, is analyzed. Figure 4 presents such a semi logarithmic plot of electronic current dependence on V_b in LabView software. The plot shows clearly a two-slope linear dependence. At low values of the probe retarding potential (V_b), which corresponds to low values of electron kinetic energy, the slope of the linear dependence of $\ln(I_e)$ on V_b is larger and corresponds to low value of secondary electron temperature, T_s. At large value of

V_b, the slope of the linear dependence of ln(I_e) on V_b is smaller and corresponds to the larger value of primary electron temperature, T_p. However, the slope values of linear dependence of ln(I_e) on V_b in the two regions do not give accurate values of T_s and T_p. because the contributions of the two electron populations on I_e are not taken separately. Therefore, an iteration algorithm is applied to separate the contribution of the two electron populations to the total electronic current. The iteration algorithm is represented in Fig. 5. In the first step of the algorithm, the values of T_{s1} and I_{s01} are determined from the slope of linear dependence of ln(I_e) on V_b in the region of low values of the retarding biasing potential [-1V; 0V]. Then the value I_{s01} and T_{s1} are used to determine $I_s(V_b)$ as $I_{0s} \cdot \exp(eV_b/k_B T_s)$ and the component $I_p(V_b)$ is determined as $I_e(V_b) - I_s(V_b)$. Then, the linear dependence of ln(I_p) on V_b is used to compute the values I_{p1} and T_{p1} corresponding to the primary electron population. In the next step of the iteration, these values are used to compute $I_p(V_b)$ as $I_{0p} \cdot \exp(eV_b/k_B T_p)$ in order to determine the $I_s(V_b)$ as $I_e(V_b)$-$I_p(V_b)$. The result is used to compute the values I_{s2} and T_{s2}, which are then used to compute I_{p2} and T_{p2}. And the algorithm may continue until the values of I_{s0}, I_{p0}, T_s, and T_p converge. Table 1 presents the values obtained along three steps of the iteration for the I-V probe characteristic presented in Fig. 5.

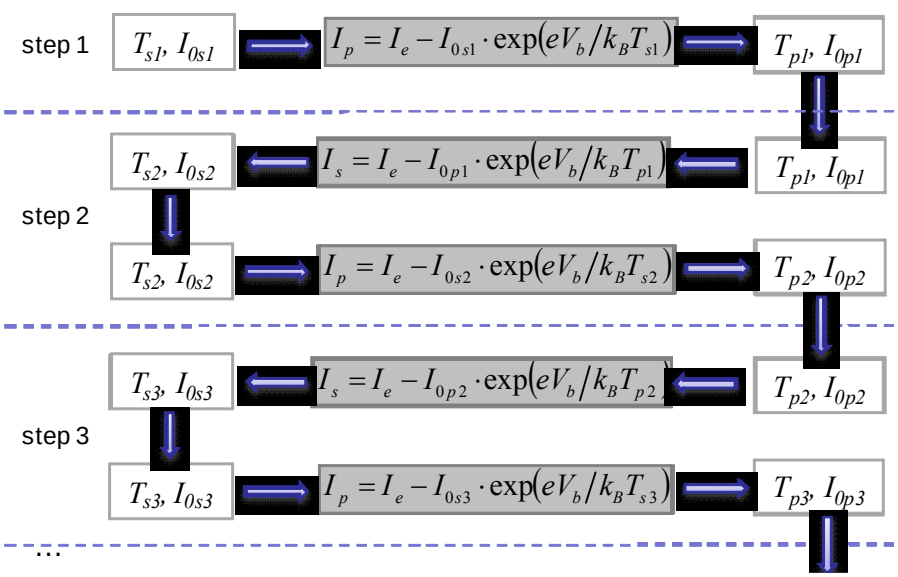

Fig. 5. Three steps of the algorithm used to separate the contributions of the primary and secondary electron populations from the total electronic current of the probe, I_e. The algorithm determines the temperature and saturation current values of the two electron populations, T_p, T_s, I_{0p}, and I_{0s}, respectively.

.

Number of iterations	Primary electrons	Secondary electrons
step 1	I_{0p1} = 0.0338 mA T_{p1} = 1.267 eV	I_{0s1} = 0.4069 mA T_{s1} = 0.212 eV
step 2	I_{0p2} = 0.0327 mA T_{p2} = 1.283 eV	I_{0s2} = 0.3837 mA T_{s2} = 0.2185 eV
step 3	I_{0p3} = 0.0291 mA T_{p3}= 1.393 eV	I_{0s3} = 0.3412 mA T_{s3} = 0.2311 eV
step 4	...	...

Table 1. Example of T_e and I_{e0} values found after 3 iterations leading to separation of the two electron populations and accurate characterization of the electrons in multi polar magnetically confined plasma.

References

[2.1] J. D. Swift and M. J. R. Schwar, *Electrical Probes for Plasma Diagnostics,* (Iliffe, London, 1970).

[2.2] N. Hershkowitz, in *Plasma Diagnostics*, edited by O. Auciello and D. Flamm (Academic, New York, 1989), Chap. 3.

[2.3] M. J. Druyvesteyn, Z. Phys. **64**, 781 (1930).

[2.4] F. F. Chen,

[2.5] M. B. Hopkins and W. G. Graham, J. Phys. D **20**, 838 (1987).

[2.6], E. Stamate, G. Popa, and K. Ohe, Rev. Sci. Instrum. **70** 58 (1999).

[2.7]Y. Ghim(Kim), N. Hershkowitz, Rev. Sci. Instrum. **80** 033502 (2009).

PRACTICUM 2

Determination of electron energy distribution function by Druyvesteyn method

D. Alexandroaiei

Introduction

In the practicum 1 one has established that the Langmuir probe electronic current is a function of the probe retarding biasing voltage, V, which is measured with respect to the plasma potential V_p ($V = V_b - V_p$, where V_b is the probe biasing potential). Having in mind that an electron from the surrounding plasma can reach the probe surface if its kinetic energy exceeds the electrostatic energy at the entrance in the probe space charge sheath:

$$m_e v_n^2 / 2 \geq eV, \qquad (1)$$

it results that the probe electronic current intensity is a function of this voltage, $I_e = I_e(V)$. More precisely, the electronic current variation dI_e, for an interval of the biasing voltage [V, $V + dV$], corresponds to an interval of velocities [v_n , $v_n + dv_n$] and, of course, to a variation of the number density corresponding to this,

$$dn_n = f_e(v_n) \cdot dv_n ,$$

where $f_e(v_n)$ is the electron velocity distribution function (EVDF). As it was discussed above, we can write:

$$dI_e = eA_P \cdot v_n dn_n, \qquad (2)$$

and this shows that there is a connection between the derivative of Langmuir probe current-voltage characteristic (dI_e/dV) and the EVDF:

$$I_e(V) = eA_P \cdot \int_{v(V)}^{\infty} v_n \cdot f_e(v_n)\, dv_n , \quad \text{where } v(V) = (2 \cdot eV/m_e)^{1/2} \qquad (3)$$

For a probe which is not plane and for isotropic plasmas one has to reconsider the condition (1) for the electrons because they come from all directions of the semi-space in front of the probe (taken to be small) and one have to take in consideration a three-dimensional EVDF. Now, the information on EVDF is contained in the current-voltage probe characteristics, $I_e = I_e(V)$, but in a more complicated mode. For this case Druyvesteyn has shown that EVDF, $f(v)$, is proportional to the second derivative of the I-V probe characteristic, $I_e = I_e(V)$ [1]. This fact is demonstrated in the following.

Theoretical Background

1. *The electronic probe current for a retarding-electron voltage*

When discussing about an isotropic plasma, we are discussing about an isotropic electronic velocity distribution function (EVDF), which is $f(\vec{v}) = f(v,\theta,\varphi)$ in spherical coordinates or $f(\vec{v}) = f(v_x, v_y, v_z)$ in rectangular coordinates. In the case of the isotropic plasmas the distribution function does not depend on the angles θ and φ, namely $f(\vec{v}) = f(v)$.

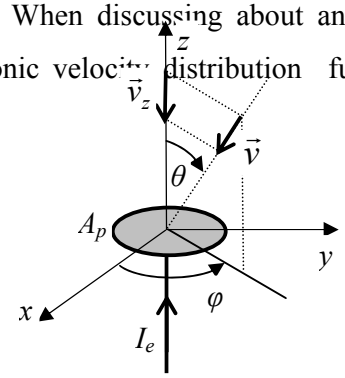

Fig.1. Geometry of electron movement in the probe sheath.

Considering that for a retarding probe potential V, with respect to plasma potential, the electrons can reach the probe surface if

$$\frac{1}{2}m_e v_z^{\,2} = \frac{1}{2}m_e v^2 \cos^2\theta \geq eV\,, \qquad (4)$$

the total current of the electrons that are collected by probe [2-5], is

$$I_e = -A_p \cdot e \cdot \Phi_{ez} = -A_p \cdot e \cdot \iiint v_z \cdot f(v) \cdot v^2 \sin\theta \cdot d\theta \cdot d\varphi \cdot dv\,, \qquad (5)$$

where Φ_{ez} is the electronic flux in the Oz direction which is perpendicular to the probe surface (see Fig.1):

$$\Phi_{ez} = \int_0^{2\pi} d\varphi \int_0^{\theta_V} \cos\theta \cdot \sin\theta \cdot d\theta \cdot \int_{v_{0z}}^{\infty} v \cdot f(v) \cdot v^2 \cdot dv\,.$$

The velocity v_z is the projection of the electron velocity on the axis Oz, $v_z = v \cdot \cos\theta$ (see Fig.1), θ_V, is the maximal limit of θ angle at which, for a given value of V, the plasma electrons having the initial velocity v arrive on the probe surface with a zero velocity. From the condition (4), it results that $\cos\theta_V = \sqrt{2e \cdot V / m_e \cdot v^2}$ .The integration limit v_{0z} for the variable v is the lowest value of the plasma-electron velocity, $v_{0z} = \sqrt{2eV / m_e}$, which corresponds to $\theta = 0$.

Integrating the equation (5) along φ and θ results in :

$$\int_0^{2\pi} d\varphi = 2\pi\ , \quad \int_0^{\theta_V} \cos\theta \cdot \sin\theta \cdot d\theta = \int_\theta^{\theta_V} \sin\theta \cdot d\sin\theta = \frac{1}{2}\sin^2\theta\Big|_0^{\theta_V} = \frac{1}{2}\left(1-\cos^2\theta\right)\Big|_0^{\theta_V} = \frac{1}{2}\cdot\left(1-\frac{2eV}{m_e v^2}\right),$$ and

Becomes:

$$I_e = -A_p \cdot e \cdot 2\pi \cdot \frac{1}{m_e^2} \cdot \int_{eV}^{\infty} f(v) \cdot \left(1 - \frac{2eV}{m_e v^2}\right) \cdot m_e v^2 / 2 \cdot d(m_e v^2 / 2)$$

By changing of the variable velocity, v, with the kinetic energy E_c, $E_c = \frac{1}{2} m_e v^2$, the electronic probe current for the retarding probe voltage, V, becomes:

$$I_e(V) = -A_p \cdot \frac{2\pi \cdot e}{m_e^2} \cdot \int_{eV}^{\infty} (E_c - e \cdot V) f(E_c) \cdot dE_c \qquad (6)$$

where $f(E_c)$ is the EVDE, $f(v)$, in which v is replaced with $(2E_c/m_e)^{1/2}$.

Observation 1:

If one takes $f(E_c) = n_0 \left(\frac{m_e}{2\pi k T_e}\right)^{3/2} \cdot \exp\left(-\frac{E_c}{kT_e}\right) = f_0(E_c)$, namely it is assumed a Maxwell distribution function for plasma electrons, by resolving (6) it is obtained the expression of the electronic probe current described in Practicum 1:

$$I_e = I_{e0} \cdot \exp\left(-\frac{eV}{kT_e}\right), \qquad (7)$$

where $I_{e0} = -\frac{1}{4} A_p \cdot e \cdot n_0 \cdot \sqrt{\frac{8kT_e}{\pi \cdot m_e}}$.

2. Determination of electron energy distribution function

The probe current (6) it described mathematically by the fallowing generic equation:

$$G(x) = \int_{g(x)}^{\infty} F(x, y) \cdot dy, \qquad (8)$$

and its derivative is:

$$\frac{dG}{dx} = \int_{g(x)}^{\infty} \frac{\partial F}{\partial x} \cdot dy - \frac{dg}{dx} F(x, y)\Big|_{y=g(x)}. \qquad (9)$$

Where $G(x) = I_e(V)$, $\mathrm{F(x, y) = (E_c - eV) \cdot f(E_c)}$; $\mathrm{E_c = y}$; $\mathrm{x = V}$; $\mathrm{g(x) = e \cdot V}$.

Therefore, the first derivative of the $I_e - V$ characteristic is:

$$\frac{dI_e}{dV} = -\frac{2e\pi \cdot A_p}{m_e^2} \left[\int_{eV}^{\infty} f(E_c) \cdot (-e) \cdot dE_c - e \cdot f(E_c)\Big|_{E_c = eV} \cdot 0 \right], \qquad (10)$$

while the second derivative is:

$$\frac{d^2 I_e}{dV^2} = \frac{d}{dV}\left(\frac{dI_e}{dV}\right) = \frac{2e^2\pi \cdot A_p}{m_e^2} \left[\int_{eV}^{\infty} 0 \cdot dE_c - e \cdot f(E_c)\Big|_{E_c = eV} \right] \qquad (11)$$

From (11) we find the EVDF as:

$$f(E_c)\big|_{E_c=eV} = \frac{-1}{2e\pi \cdot A_p} \cdot \left(\frac{m_e}{e}\right)^2 \cdot \frac{d^2 I_e}{dV^2} \qquad (12)$$

Observation 2:

Having the electron velocity distribution function, $f(v)$, which was transformed in $f(E_c)$ as it was shown before ($v = (2E_c/m_e)^{1/2}$), we can obtain the electron energy distribution function (EEDF), $f_E(E_c)$, by using the fallowing conversion relation:

$$dn = 4\pi v^2 \cdot f(v) \cdot dv = f_E(E_c) \cdot dE_c \,,$$

where $f_E(E_c) \cdot dE_c$ is the electron number with $v \in [v\,,\ v+dv]$ and $E_c \in [E_c\,,\ E_c+dE_c]$ with $dv/dE_c = (2E_c/m_e)^{-1/2}$. Therefore, the EEDF, $f_E(E_c)$, is:

$$f_E(E_c)\big|_{E_c=eV} = \frac{-4}{e^2 A_p} \cdot \sqrt{\frac{m_e \cdot V}{2e}} \cdot \frac{d^2 I_e}{dV^2} \qquad (13)$$

Observation 3:

The EEDF at $E_c = 0$ is zero, therefore the second derivative of the $I_e = I_e(V)$ is null in V = 0, which is at $V_b = V_p$. This means that V_p is the probe bias voltage for which the second derivate of the $I_e = I_e(V)$ is zero or its first derivate, $d\,I_e/dV$, has the maximal value [5].

Experiment

Figure 2 presents a probe I-V characteristic and its first and second derivatives for a cylindrical Langmuir probe (tungsten wire with 0.3 mm in diameter and 5 mm in length) in the multipolar magnetically confined plasma obtained by electrical discharge (discharge current intensity of 100 mA, and discharge voltage of 70 V) in air at pressure of 10^{-4} Torr. The multipolar magnetically confined plasma device, the data acquisition system of the probe I-V characteristics and the digital data processing software are described in Annexes. The probe current and biasing voltage data are stored in a file (CSV type) and processed by a specialized homemade software in LabView. The first and second derivative of the $I(V)$ are computed locally [5], in each point of the I-V characteristic, by fitting of the characteristic on a small interval of biasing voltage values centered on the reference point by a second grade polynomial function (see Fig. 3)

A first question concerning the derivative computation is the fact that for bias voltages in the retarding-electrons region the probe current contains both by the electronic and the ionic current:

$$I = I_e + I_i$$

In practice, because $I_e >> I_i$ and I_i has a very weak dependence on V, it is not necessary to subtract the ion component of the probe current before computing the derivatives.

Another question is the presence of the plasma noise which can affect the probe characteristic and the derivatives. Analogical circuits can be used to prevent or to stop the influence of the noise or in the case that it is presented noise-suppression techniques are used for smoothing the *I-V* characteristic.

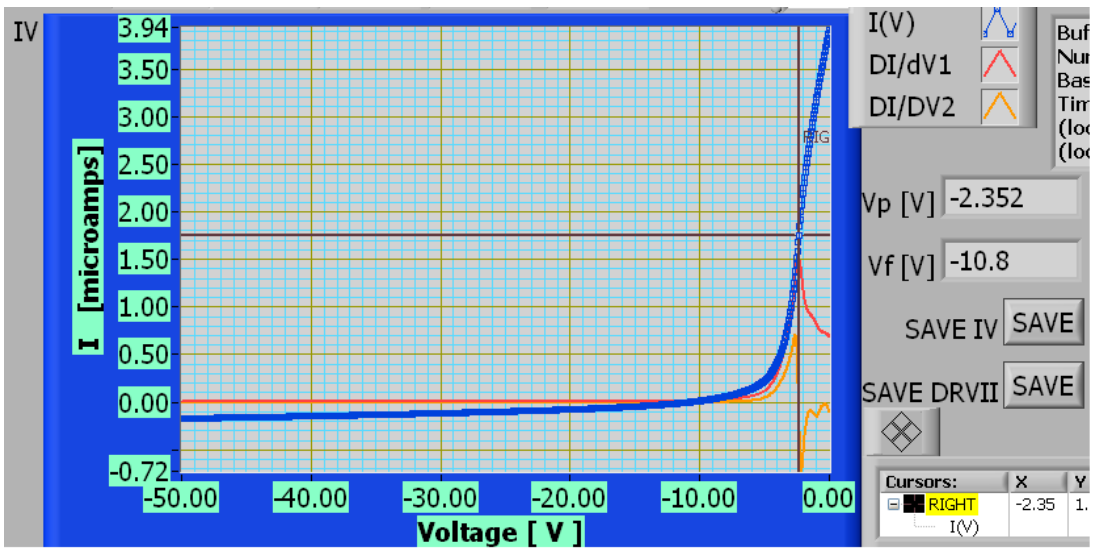

Fig. 2 Probe I-V characteristic and its derivatives. Plasma potential is determined as the biasing potential at which dI/dV is maximum or at which dI/dV = 0.

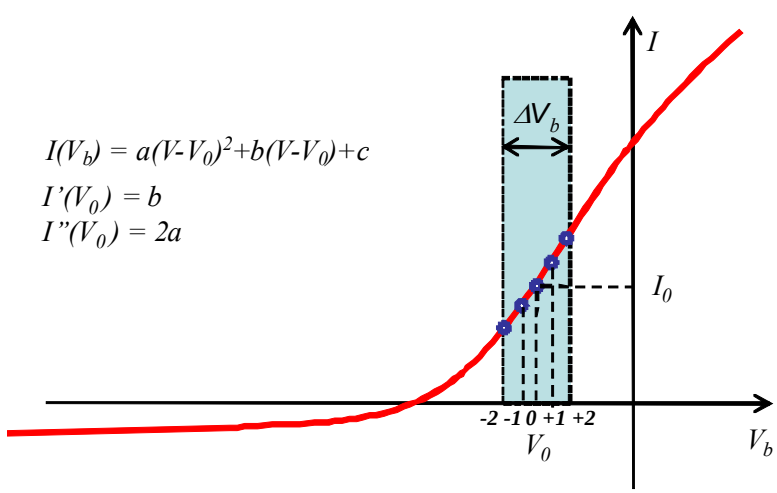

Fig. 3 Computing the local value of I(V) derivatives by polynomial fitting of a small portion of the I-V curve. The fitting interval, ΔV, determine the energy resolution of the EEDF.

a)

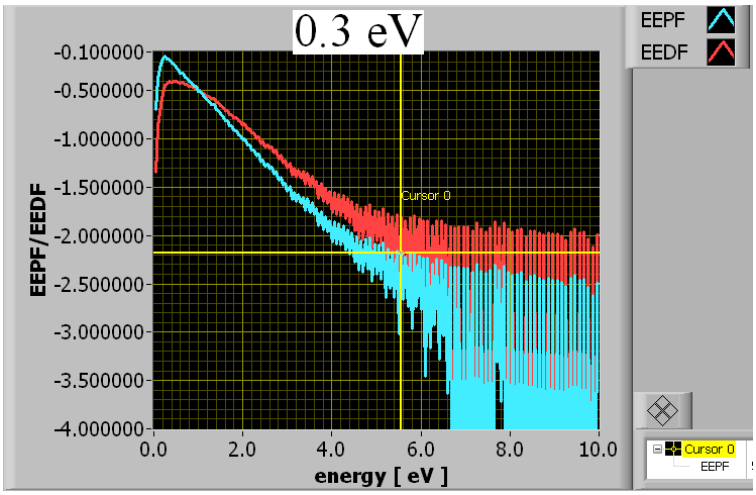

b)

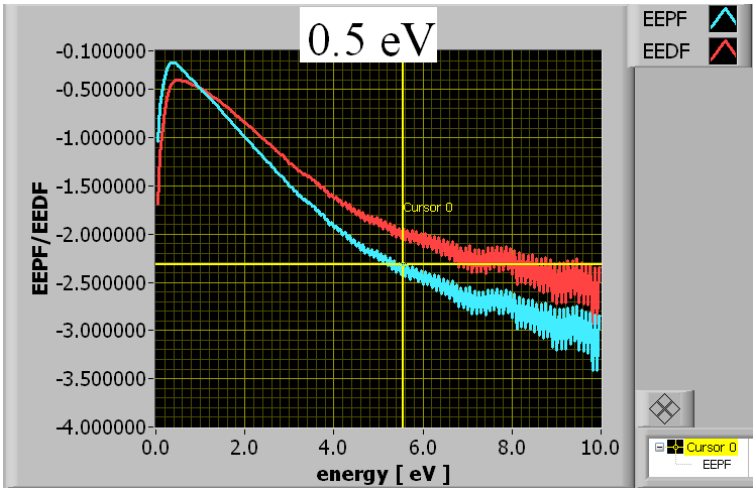

c)

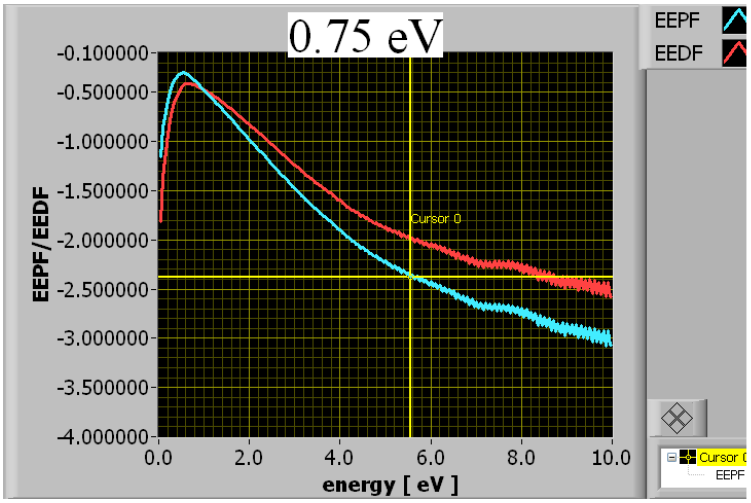

Fig. 4 EEDF and EEPF computed with different energy resolutions. a) $\Delta E = e \cdot \Delta V = 0.3$ V; b) $\Delta E = e \cdot \Delta V = 0.5$ V; a) $\Delta E = e \cdot \Delta V = 0.75$ V;

Figure 4 shows the EEDF and EEPF computed with different energy resolutions, *i. e.* different values of polynomial fitting interval, ΔV. Increasing of the smoothness of second probe derivative is done with the expense of the loosing energy resolution. At high energy resolution the noise is dominant in the energetic tail of the EEPF, fact which discards the data obtained in this region.

References:

[1] M J Druyvesteyn, Z. Phys. **64** (1930) 781

[2] N Hershkowitz, *Plasma Diagnostics*, Vol. 1 Ed. Orlando Auciello and Daniel L Flamm, Academic Press, Inc. Boston San Diego, (1989), Chap. 3, p. 114

[3] J D Swift, M R J Shwar, *Electrical Probe for Plasma Diagnostics* – ILLFE- Book (1970)

[4] F.F.Chen, *Langmuir Probe Diagnostics*, Mini-Course on Plasma Diagnostics, IEEE-ICOPS meeting, Jeju, Korea, June 5, 2003

[5] G.Popa, L.Sirghi *Basic of Plasma Physics*, Ed. "Al.I.Cuza" University Press, Iasi, Romania, (2000) (in romanian)

[6] G.Popa, D.Alexandroaei, *Guide of Practical Work for Plasma Physics* Ed. "Al.I.Cuza" University Press, Iasi, Romania, (1991), (in romanian)

PRACTICUM 3

Dependence of ion and electron saturation currents on probe geometry

L. Sirghi

Introduction

As it has been described in practicum 1, the theoretical probe I-V characteristic in a homogeneous plasma has an electron saturation region, when the probe is biased positively with respect to plasma potential, V_p, and the probe current is constant and equal to the electronic saturation current of the probe, I_{e0}, and a ion saturation region, when the probe is biased negatively with respect to V_p and the probe current is constant and equal to the ion saturation current of the probe, $-I_{i0}$. However, in practice the probe current intensity in the saturation regions is not constant. Figure 1 presents a real probe I-V characteristic that shows in the electron saturation region ($V_b > V_p$) a continuous increase of the probe current with the increase of V_b. On the other hand, in the ion saturation region ($V_b << V_p - kT_e/e$) the ion current continues to increase with the decrease of V_b. In order to understand why this is happening, we have to consider the probe geometry effect on the area of charge collection surface of the probe.

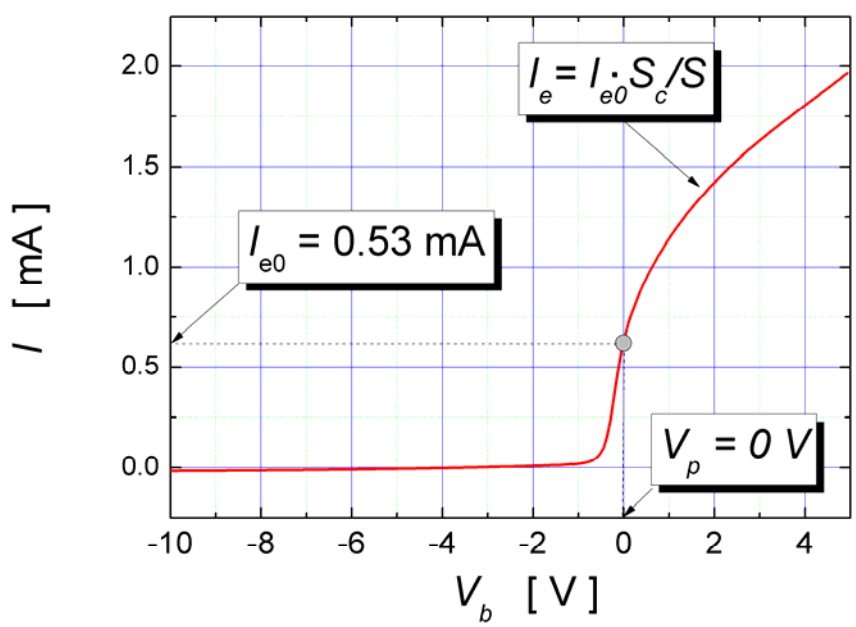

Fig. 1 A real probe IV characteristic showing a continuous increase of current intensity in the electronic saturation region ($V_b > V_p$, $V_p = 0$).

An electrically biased probe is usually separated by plasma by a space charge sheath of which thickness, d, determines the area of the charge collection surface (Fig. 2). In the practicum 1 d is considered negligible small by comparison to the probe dimension. In this case, the charge collection surface of the probe, S_c, has approximately the same area as the active surface of the probe, S (Fig. 2 A). On the other hand, if d is comparable with the probe dimension, S_c is larger than S (Fig. 2B). The geometry of the probe is important, the effect being more important for spherical or cylindrical probes than for planar probes (Fig. 2C). As d depends on V_b, S_c continues to increase with $|V_b - V_p|$ with the result of increasing of the intensity of saturation probe currents. Thus, the probe current intensity in the electron and, respectively, ion saturation regions is:

$$I = I_{e0} \cdot S_c(V_b)/S \text{ for } V_b > V_p \tag{1a}$$

$$I = -I_{i0} \cdot S_c(V_b)/S \text{ for } V_b << V_p - kT_e/e, \tag{1b}$$

where

$$I_{e0} = S \cdot j_{0e} = S \cdot \frac{1}{4} e \cdot n_e < \mathrm{v}_e > = e \cdot n_e \cdot S \cdot \sqrt{\frac{k_B T_e}{2\pi m_e}}, \tag{2a}$$

$$I_{i0} = S \cdot j_{0i} = S \cdot \frac{1}{4} e \cdot n_i < \mathrm{v}_i > = e \cdot n_i \cdot S \cdot \sqrt{\frac{k_B T_i}{2\pi m_i}}, \tag{2b}$$

and j_{0e} and j_{0i} are the thermal densities of electron, respectively, ion currents in plasma.

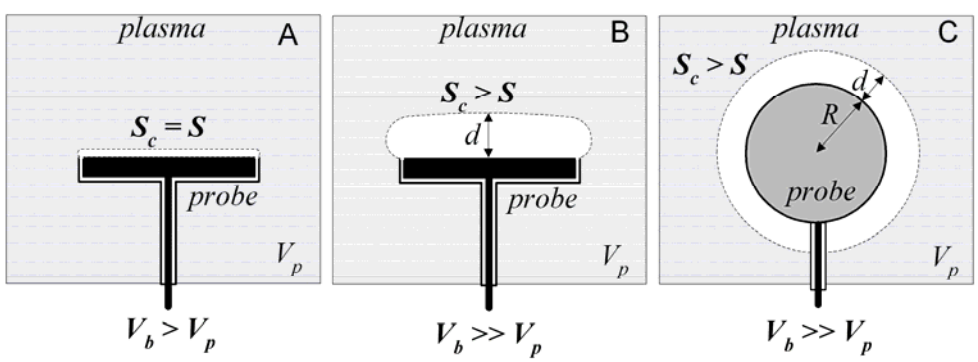

Fig. 2 Variation of the area of charge collection surface, S_c, of an electrical probe in the electron saturation regime ($V_b > V_p$). A: The thickness of the space charge sheath between the probe and plasma, d, is much smaller than the probe dimension and $S_c \cong S$; B: At large values of V_b ($V_b - V_p >> kT_e/e$) The thickness of the space charge sheath between the probe and plasma is comparable with the probe dimension and $S_c > S$; C: The effect of increasing of S_c depends on the probe geometry, it being stronger for cylindrical or spherical probes by comparison to the effect for the planar probe.

The thickness of the probe sheath, d, depends on how strongly is biased the probe against the plasma, *i. e.* $|V_b\text{-}V_p|$. Naturally, d increases with the increase of $|V_b\text{-}V_p|$, with the effect of increase of S_c. This increase of S_c determines the increase of probe saturation current in the electron regions as it is shown by the probe I-V characteristic presented in Fig. 1.

Theory

The thickness of the probe sheath, d, is usually approximated by the plasma Debye length,

$$\lambda_D = \sqrt{\frac{\varepsilon_0 \cdot kT_e}{n \cdot e^2}}, \qquad (2)$$

where n is the plasma density, e the elementary electric charge, and T_e, the electron temperature. This approximation works well for weakly biased probe (for $|V_b - V_p| \cong kT_e/e$), but underestimate seriously the value of d for strongly biased probe (for $|V_b - V_p| >> kT_e/e$). Using the Bohm current intensity for the ion saturation current intensity in the Child-Langmuir equation for a strongly (negative) biased probe, the fallowing equation for d is obtained[4.1]:

$$d \approx \lambda_D \cdot \left[\frac{e(V_p - V_b)}{kTe}\right]^{3/4} \qquad (3).$$

Thus, for a probe biased at $V_p\text{-}V_b = 10 \cdot kT_e/e$, $d \cong 6 \cdot \lambda_D$. This result shows that the probe sheath can be one order of magnitude larger than the Debye length.

It is difficult to establish an analytical expression of variation of S_c with V_b for a planar probe. R Sheridan [4.2] has proposed the fallowing empirical dependence S_c on on V_b for a small planar disk probe:

$$S_c = S \cdot (1 + a \cdot \eta^b), \qquad (4)$$

where $\eta = e(V_p - V_b)/kT_e$. The fitting parameters a and b for $5 < \eta < 30$ and $R < 45 \cdot \lambda_D$ are given by:

$$a = 2.28 \cdot (R/\lambda_D)^{-0.749}, \qquad (5a)$$

and

$$b = 0.806 \cdot (R/\lambda_D)^{-0.0692}. \qquad (5b)$$

Here λ_D is the Debye length and R, the radius of the planar disk probe.

For cylindrical and spherical probes, the effect of probe geometry on the behavior of the probe I-V characteristic in the saturation regions is described well by the single particle orbital theory developed by Langmuir and Mott-Smith [4.3]. This theory considers the ballistic movement (without collisions) of charged particles in the attractive electric field of

the probe sheath (Fig. 3), movement that obey the energy and angular momentum conservation laws. Thus, the fate of attracted charged particles entering from the unperturbed plasma at the electric potential V_p in the field of the probe sheath depends on particle velocity v_0 and impact parameter, p, at the moment of entrance. Particles coming into the sheath with large v0 and p will be deviated, but not collected by the probe. For a certain value of v_0 there is a critical value of p, p_c, for which the charged particle reaches the probe surface. To derive an expression of p_c, the particle energy and angular momentum conservation lows are written for critical particle trajectory (see Fig. 3) as it fallows:

$$\frac{m\mathrm{v}_0^2}{2} + q \cdot V_p = \frac{m\mathrm{v}^2}{2} + q \cdot V_b \tag{6}$$

and

$$m\mathrm{v}_0 \cdot p_c = m\mathrm{v} \cdot R\,. \tag{7}$$

Simple algebra operations lead to the fallowing expression of p_c:

$$p_c = R \cdot \sqrt{1 + \frac{2q(V_p - V_b)}{m\mathrm{v}_0^2}} \tag{8}$$

Considering that all the ions that are collected by the biased probe enter in the probe sheath with the same initial velocity, v_0, the fallowing expressions of the probe saturation ion current intensity are found for cylindrical and, respectively, spherical probes:

$$I_i = q \cdot n \cdot \mathrm{v}_0 \cdot 2\pi p_c \cdot l = j_{i0} \cdot 2\pi R \cdot l \cdot \sqrt{1 + \frac{2q(V_p - V_b)}{m\mathrm{v}_0^2}} = I_{0i} \cdot \sqrt{1 + \frac{(V_p - V_b)}{V_0}} \tag{9}$$

$$I_i = q \cdot n \cdot \mathrm{v}_0 \cdot 4\pi\, p_c^2 = j_{i0} \cdot 4\pi R^2 \cdot \left(1 + \frac{2q(V_p - V_b)}{m\mathrm{v}_0^2}\right) = I_{0i} \cdot \left(1 + \frac{V_p - V_b}{V_0}\right). \tag{10}$$

However, the real movement of particles in the probe sheath is more complicated because not all particles have the same initial velocity v_0 at the entrance into the probe sheath. Langmuir and Mott-Smith considered a Maxwellian velocity distribution of v_0, which resulted in more complicated expressions for the probe saturation current in the saturation regions [1]. However, for thick probe sheaths ($d > R$) the equations (9) and (10) can be applied for Maxwellian plasma particles by taking the expressions (2a) and (2b) for the probe saturation current intensities I_{0e} and I_{0i} and the thermal velocity for v_0 [1]. Thus, $V_0 = kT_{e,i}/e$. Equations (9) and (10) apply as well for the electron saturation current.

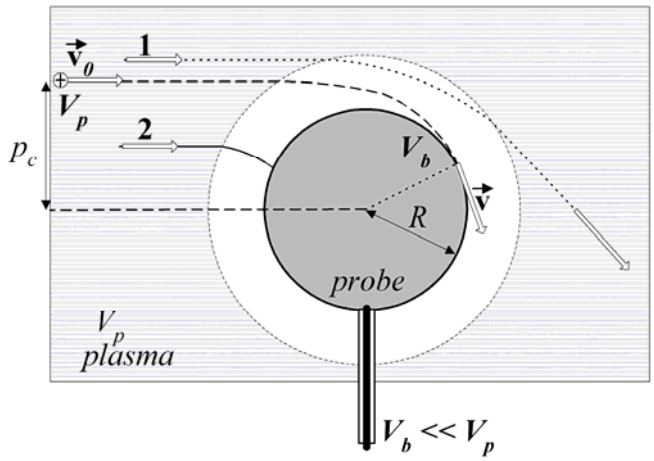

Fig. 3 Ballistic motion of ions in the radial electric filed of the probe sheath of a strongly (negative) biased cylindrical or spherical probe. All ions coming to the probe with $p < p_c$ are collected by the probe surface (trajectory "2"). All ions coming to the probe sheath with p > pc are escaping the attractive field of the probe sheath. Particle coming to the probe sheath with $p = p_c$ collide the probe surface tangentially.

Experiment

The experiments are performed in multi polar magnetically confined plasma device in argon plasma at pressure ranged between 10^{-4} to 10^{-3} Torr. A cylindrical probe with length of 5 mm and diameter of 0.3 mm is installed in the center of the plasma chamber along its axis. Before measurements, the probe is cleaned by electron bombardment. Then, the I-V probe characteristics are acquired and processed by specialized homemade software in LabView. The goal of the experiment is to investigate the dependence of probe current on V_b in the probe electron and ion saturation regions.

First step in data processing consist in determination of plasma potential, V_p, and taking the value of V_p as reference for V_b (which means that the I-V probe characteristic is shifted on the potential axis so that $V_p = 0$). As in the practicum 1, the value of V_p is determined by the maximum of first derivative of the probe current, $I' = dI/dV_b$.

Next step in data analysis is to examine the dependence of square of I on V_b. Since for the cylindrical probe a dependence of the probe current intensity on the square root of $1+e|V_b|/kT$ is expected in the saturation regions. Figure 4 presents an image of the front panel of the LabView data processing program used to analyze the single probe I-V characteristics in the electron and ion saturation regions. The upper graph is used to determine the values of plasma and floating potentials, while the bottom graph of $I^2(V_b)$ is used to examine the behavior of I-V characteristic in the electron saturation region. As expected, the dependence

of I^2 on V_b in this region is linear and a linear fit of data provide values for I_{e0} and T_e. The obtained values of I_{e0} and T_e can be compared with the electron saturation current and electron temperature obtained in Practicum 1. The front panel has a similar graph for analysis of the probe ion saturation region (not shown). This graph of $I_2(V_b)$ is used to determine the Bohm velocity (or the ion temperature in hot plasmas) of ions and the ion saturation current, I_{i0}. However, this analysis does not work for the multi polar magnetically confined plasma, the value of I_{i0} being negative. A possible cause of this may be the effect of energetic particles (electrons) on the probe sheath.

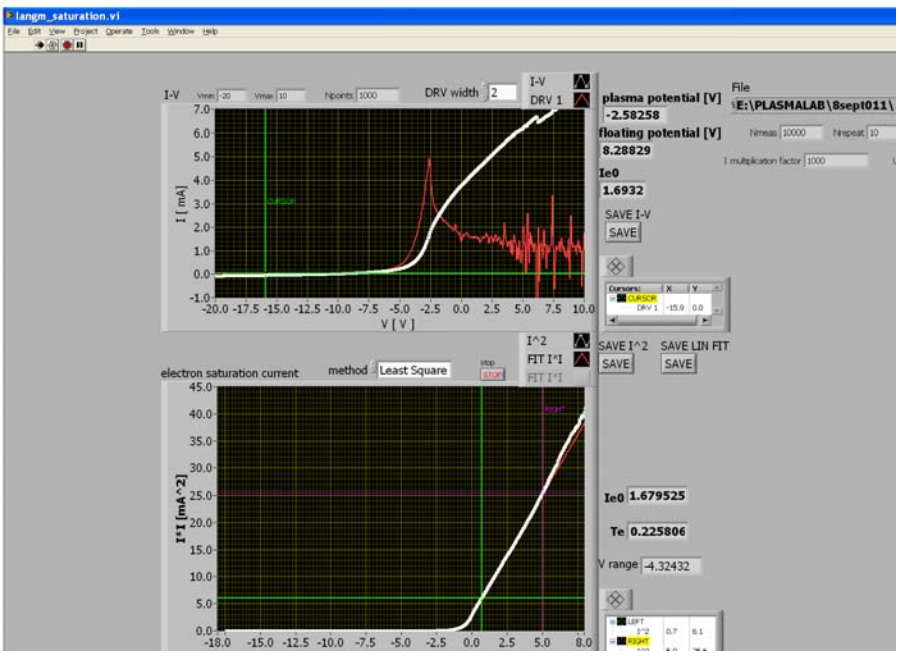

Fig. 4. Example of data processing by a dedicated LabView software used for analysis of the single probe I-V characteristic in the electron saturation region. The square of the probe electronic current increases linearly with the increase of V_b for $V_b > 0$.

References

[4.1] N. Hershkowitz, How Langmuir probes works, p. 131
[4.2] T. E. Sheridan, Phys. Plasmas **7**, 3084 (2000)
[4.3] I. Langmuir, H. M. Mott-Smith, Gen. Elec. Rev. **27**, 449,583, 616,726, 810 (1924)

PRACTICUM 4

Double electrical probe I-V characteristics in homogeneous plasmas. Measurement of the electron temperature and density

C. Costin

Purpose

The purpose of this practical work is the measurement of electron temperature and plasma density by means of double probe.

Theoretical background

In some cases the simple electric probe (also called Langmuir probe) can not be used for plasma local diagnosis (such as the case of plasmas without reference electrodes, plasma regions with very high electric potential with respect to a reference electrode, cosmic plasmas, etc) and it can be replaced by the double probe.

A double probe consists of two single probes, in most of the cases identical, introduced in plasma at a relatively small distance one to each other. This distance must be greater than the sheath regions of the two probes, but smaller than the typical dimension of plasma inhomogeneity. A power supply is connected between the two probes (outside the plasma), in order to bias one of them with respect to the other. A mili- or micro-amperemeter can be used for current measurements while a voltmeter can indicate the biasing voltage (see Fig.1).

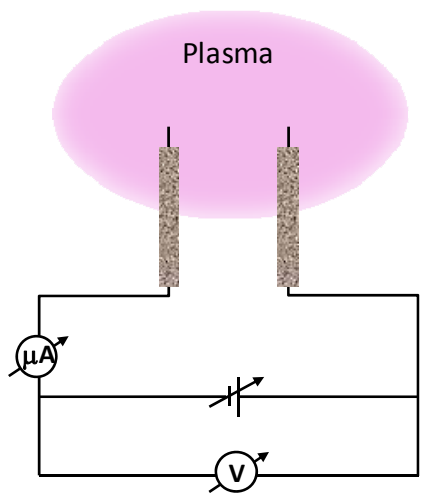

Fig.1. Scheme of the double probe circuit

In order to understand the principle of the double probe some assumption has to be made: (*i*) homogeneous and collisionless plasma and (*ii*) all assumptions for the Langmuir probe are valid.

The theory is similar to that of a Langmuir probe, except that the current is limited to the ion saturation current for both positive and negative voltages.

When the two probes are floating, both of them will be negatively charged with respect to plasma at the floating potential

$$V_f = V_p - \frac{k_B T_e}{2e} \ln\left(\frac{T_e m_i}{T_i m_e}\right)$$

where V_f is the floating potential, V_p – plasma potential, $T_{e,i}$ – electron and ion temperature, $m_{e,i}$ – electron and ion mass, e is the elementary charge (1.6×10^{-19} C) and k_B the Boltzmann constant (1.38×10^{-23} J/K). In this case the current density through each probe is zero:

$$j = j_i + j_e = j_{oi} - j_{oe} \exp\left(\frac{e(V_f - V_p)}{k_B T_e}\right) = 0,$$

where j_{oi} and j_{oe} are ion and, respectively, electron saturation current densities given by

$$j_{oi,e} = \frac{1}{4} e n_0 \sqrt{\frac{8 k_B T_{i,e}}{\pi m_{i,e}}}.$$

Plasma density is designated by n_0 and the current density is obtained by dividing the measured current to the probe area.

By applying a biasing voltage U between the two probes, for example probe 1 more negative than probe 2, the potential of each probe will become V_1 and V_2 (Fig.2). Both probes remain at a negative potential with respect to plasma but because $V_1 \neq V_2$ a current will flow through the circuit of the two probes. Each probe will collect from the plasma a current carried by electrons and ions, corresponding to the potential difference between the probe and the plasma. As the two probes are connected in a series electric circuit, the currents collected by the two probes have to be equal in magnitude, even if one probe (1 in this case) collects more ions while the other (probe 2) collects more electrons. Thus, the current density through the electric circuit can be written:

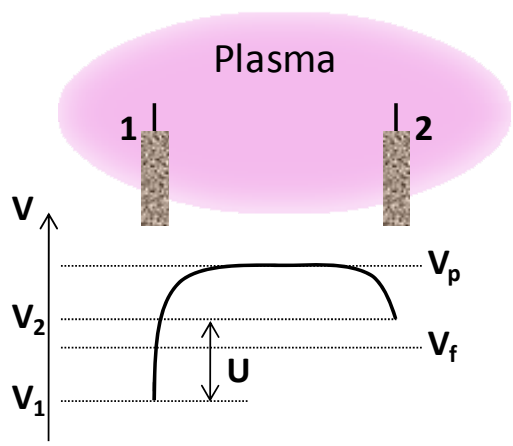

Fig.2. Potential distribution between the two probes

$$j = j_1 = j_{i1} + j_{e1} = j_{oi1} - j_{oe1} \exp\left(\frac{e(V_1 - V_p)}{k_B T_e}\right) = -j_2 = -(j_{i2} + j_{e2}) = -j_{oi2} + j_{oe2} \exp\left(\frac{e(V_2 - V_p)}{k_B T_e}\right)$$

As homogeneous plasma was assumed, then $j_{oi1} = j_{oi2} = j_{oi}$ and $j_{oe1} = j_{oe2} = j_{oe}$. The expression above can be rewritten only as a function of j_{oi} and $U = V_2 - V_1$:

$$j = j_{oi} \frac{\exp\left(\frac{eU}{k_B T_e}\right) - 1}{\exp\left(\frac{eU}{k_B T_e}\right) + 1} = j_{oi} \tanh\left(\frac{eU}{2k_B T_e}\right).$$

A typical ideal current-voltage characteristic of the double probe is plotted in Fig.3.

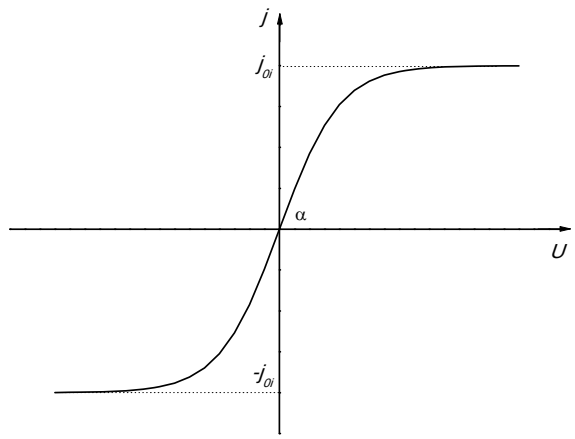

Fig.3. Ideal current-voltage characteristic of a double probe

The maximum current in the double probe's circuit is limited by the ion saturation (or thermal) current. The electron current in the double probe's circuit is given by a small fraction of electrons moving from the plasma to the probes, namely the most energetic ones. Once the ion saturation current is measured, the electron temperature can be estimated from the first derivative of the current-voltage characteristic of the double probe calculated at U = 0:

$$\left.\frac{dj}{dU}\right|_{U=0} = tg\alpha = \frac{j_{oi}}{2} \frac{e}{k_B T_e}.$$

This relation is valid only if the electron distribution function is maxwellian.

One advantage of the double probe is that neither electrode is ever very far above floating, so the theoretical uncertainties at large electron currents are avoided. If it is desired to sample more of the exponential electron portion of the characteristic, an asymmetric double probe may be used, with one electrode larger than the other. The characteristic in this case is still a hyperbolic tangent, but shifted vertically. Another advantage is that it needs no reference to the vessel. On the other hand, it shares the limitations of a single probe concerning complicated electronics and poor time resolution.

Experimental set-up

The double probe consists of two cylindrical probes made of tungsten wire (5mm in length and 0.3 mm in diameter) disposed at about 3 mm one to the other. The probes are fixed in a ceramic shaft, only the active part remaining non-isolated. For measurements, the double probe is introduced in the multi-polar confinement plasma device described in Annex 1. The circuit used for drawing the current-voltage characteristic of the double probe is almost the same as the one used for the Langmuir probe (described in Annex 2), with two differences: 1) the entire measuring system is floating and 2) the probe connector is linked to one probe and the ground connector is now linked to the second probe.

Suggestions for practicum

1. Manufacture your own double probe head. Materials needed: ceramic tube, tungsten wire, copper wire.
2. Draw current-voltage characteristics of the double probe for different plasma conditions. Determine the ion saturation current and electron temperature using the proper formula. Calculate the plasma density.
3. Obtain the double probe theory when the two probes have different areas.

PRACTICUM 5

Triple probe

G. Popa

1. Introduction

Triple probe (TP) consists of three electrical probes connected in a certain electrical circuit, which can be used for plasma diagnostic. Practically it assumes to measure potentials and currents in the circuit, which can be used for calculation of plasma parameters. Plasma parameters which can be obtained by the TP are electron temperature and electron density. Present model for data acquisition and calculation of plasma parameters with such a system is based on similar hypothesis used for classical Langmuir probe. Main advantage of such a system is that it can also be used in any un-magnetized plasma which has no inner electrode as reference for plasma potential. Moreover, it allows to measure plasma parameters in non-stationary plasma so it permits to follow plasma parameter fluctuations.

2. Theoretical model.

Let us assume the TP system made of three identical planes Langmuir probes. The probes are placed in uniform and stationary and un-magnetized plasma and the following Langmuir hypothesis are satisfied [1]:

i) the plasma is considered as mixture of three "ideal gases": electronic, ionic and neutrals. Each "gas" is characterized by its thermodynamic parameters: density and temperature as following: n_e and T_e for electrons, n_i and T_i for positive ions and n_n and T_n for neutral atoms, respectively. The neutral atoms belong to the neutral gas in which plasma state is produced. The positive ion being single ionized state of a single atomic species. Plasma is quasi-neutral so that $n_e = n_i = n_0$

ii) the plasma is non-isothermal system and electron temperature T_e is larger or even more larger than ion temperature T_i which is very close or even equal with neutral and room temperature T_n. Under such hypothesis the velocity distribution function for each sort of particles; electrons, positive ions and neutrals is a Maxwellian one:

$$f_s(\vec{v}) = n_s \left(\frac{m_s}{2\pi k T_s} \right)^{3/2} \exp\left(-\frac{m_s v^2}{2kT_s} \right) \tag{1}$$

where the index s represents: e for electrons, i for ions and n for neutrals. The m_s is

mass of a particle of sort s. The n_s and T_s have been previously defined for each sort of particles.

iii) the model is using the collisionless plasma. This assumption has to be accepted in the sense that the thickness of the space charge region around the probe is much smaller with respect to the mean free path of the particles. Consequently, any collision within the sheath region can be neglected and free fall approximation can be used for kinetic of the particles in the probe region where the electric force produced by probe potential may act on the plasma particles

iv) the probe surface is non active. It does not emit any particle of any kind and do not produce any chemical reaction.

Under these assumptions the electron and ion fluxes at the plane probe surface can be expressed analytically versus potential of the probe with respect to plasma potential.

Let us, first consider situation when all three probes are inserted in the homogeneous plasma under assumption presented above and each of them is at floating potential V_f. The floating potential V_f is negative with respect to plasma potential V_p [2]. For the sake of simplicity, let us consider the plasma potential as reference and $V_p = 0$V. In this case $V_f < 0$ and its value can be easily obtained taking into account that at floating potential the total current intensity at the probe surface is zero. Analytical expression of the floating potential is:

$$V_f = -\frac{k_B T_e}{2e} \ln\left(\frac{m_i T_e}{m_e T_i}\right) \tag{2}$$

where, besides the quantities m_s and T_s defined above there are: k_B as Boltzmann constant and e electron charge.

Next step is to consider the measuring circuit presented in Fig.1. Two *d.c.* power supplies are used to polarize the probe P1 and probe P3 negatively with respect to the probe P2. Consequently, potential V_1 of the probe P1 and potential V_3 of the probe P3 becomes more negative than floating potential and potential V_2 of the probe 2 becomes positive with respect to floating potential but it can not become positive with respect to plasma potential as is presented in Fig.1.

(Question1. *Which is the reason that V_2 can not be positive with respect to plasma potential ?).*

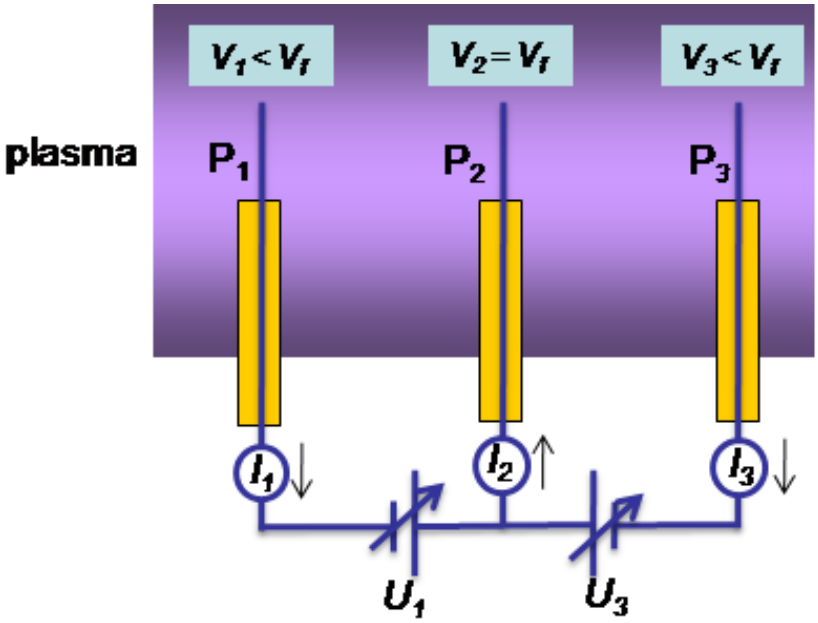

Fig.1 Principle of the Triple Probe system made of three identical plane probes and their potential with respect to plasma potential (V_p = 0V). I_i = ionic current and I_e = electron current intensity from plasma to the probe system.

In this case the intensities of the currents flowing through each probe might be express as following:

$$
\begin{aligned}
I_1 &= I_{i0} - I_{e0}\exp\left(-\frac{eV_1}{kT_e}\right) \\
I_2 &= -I_{i0} + I_{e0}\exp\left(-\frac{eV_2}{kT_e}\right) \\
I_3 &= I_{i0} - I_{e0}\exp\left(-\frac{eV_3}{kT_e}\right)
\end{aligned}
\tag{3}
$$

where, the I_{i0} and I_{e0} are the ion and electron saturation current intensities, respectively, which are given by:

$$
\begin{aligned}
I_{i0} &= \frac{1}{4} n_0 e \sqrt{\frac{8kT_i}{\pi m}} S \\
I_{e0} &= -\frac{1}{4} n_0 e \sqrt{\frac{8kT_e}{\pi m_e}} S
\end{aligned}
\tag{4}
$$

These expressions can be easily obtained under assumption that thickness of the ion sheath is very small comparing with diameter of the probe. In this case collecting area of the surface which separate unperturbed plasma and ion sheath formed in front of the negative biased probe can be considered as equal with area of the plane probe. Consequently, relations (4) besides well known quantities previously defined contain the area S of one probe, which is the same for each probe.

(Question 2: Please comment the approximation proposed. Which quantity is affected by this approximation? What other consequences of real shape of the ion sheath boundary might be considered?)

On the other hand, polarization of the probes 1 and 3 with respect to the probe 2 using the d.c. power supplies U_1 and U_3, respectively as in Fig.1 allows writing the equalities:

$$U_1 = V_1 - V_2 \qquad (5)$$

$$U_3 = V_3 - V_2$$

Using relations (3) and (5) and a simple algebra it can be obtained the following ratio:

$$\frac{I_1 + I_2}{I_3 + I_2} = \frac{1 - \exp\left(-\frac{eU_1}{kT_e}\right)}{1 - \exp\left(-\frac{eU_3}{kT_e}\right)} \qquad (6)$$

The ratio (6) includes the electron temperature T_e as one of desired plasma parameter, which can be calculated knowing the electrical tensions U_1 and U_3 and measuring the all three probe currents I_1, I_2 *and* I_3, respectively.

Once electron temperature T_e is known, another simple algebra on the same relations (3) and (5) may allow finding the ion saturation current intensity of the probe as:

$$I_{i0} = \frac{I_1 - I_3 \exp\left[-\frac{e}{kT}\Delta U\right]}{1 - \exp\left[-\frac{e}{kT}\Delta U\right]} \qquad (7)$$

Expression which include the quantity:

$$\Delta U = V_1 - V_3 = U_1 - U_3$$

and the ion saturation current intensity I_{i0}, respectively, which allows to calculate the plasma density using Bohm criteria [3] and surface area S of the plane probe:

$$n_0 = \frac{I_{i0}}{S}\frac{1}{e}\sqrt{\frac{m_i}{kT_e}} \qquad (8)$$

The model proposed can be used also for any type of probes, plane, cylindrical or spherical. The differences consist of analytical expression of the ion and electron current collected by the probes. Fortunately, under Maxvellian distribution function of the electrons the analytical form of the electron current for retarding potential of the probe as exponential formula is still valid. The main differences related to the probe geometry consist in effective area of the collecting for both ions and electrons, so that I_{i0} and I_{e0} has to be treated differently and probe geometry is important in calculation of the plasma density only. The electron temperature can be calculated using ratio (3) for any kind of three identical probes.

3. Experimental set-up

The experimental is arranged in very suitable argon plasma produced by *d. c.* hot cathode discharge with multipolar confinement system [4]. The plasma is produced in a stainless still chamber filled with argon at the pressure in the range 5.10^{-4} to 10^{-3} mbar. The probe system consists of three almost identical cylindrical probes made of tungsten weirs of 0.3 mm diameter and 5 mm length (Fig.2)

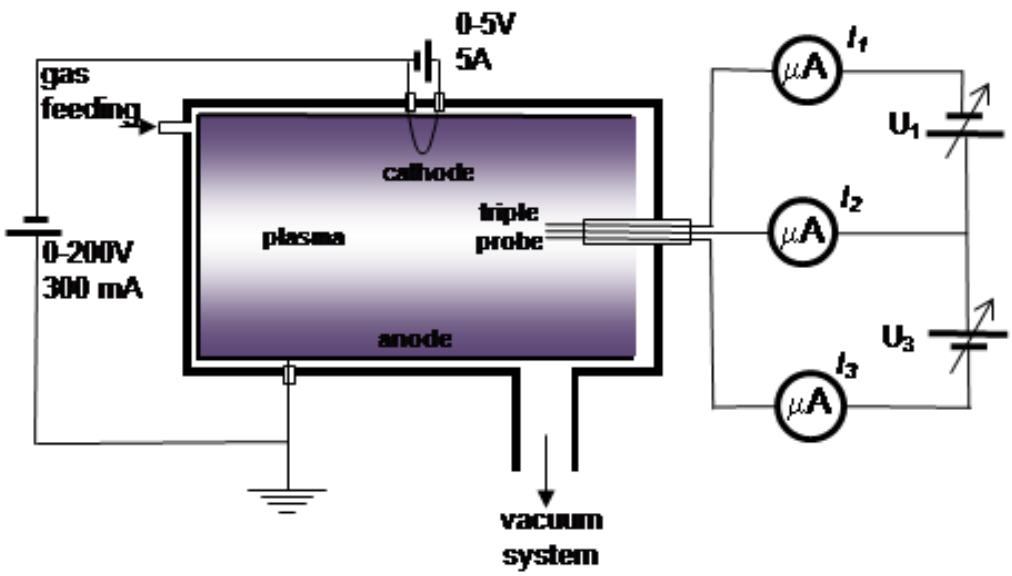

Fig. 2 Experimental set-up

(Question 3: What distance has to be considered between probes?)

i) Experiment 1.

In the first experiment is proposed to find electron temperature and density according to formulas (6) and (8). Using the experimental device presented in Fig.2 the probes current intensities I_1, I_2 *and* I_3, respectively are measured for various values of the tensions U_1 and U_3

but constant discharge parameters (constant gas pressure, discharge current intensity and discharge voltage).

(Suggestion: get series of experimental data for e.g. U_1 constant as parameter and U_3 as independent variable. Calculate the T_e and n_e and find systematic and random errors. Discuss the result).

ii) Experiment 2.

The experiment can be simplified and prepared for direct measuring of electron temperature. In order to do this it is necessary to reconsider the model described in theoretical part. Thus, let us consider that probe 3 floating and both the d.c power supply and ampermeter for I_3 replaced by a voltmeter with very high impedance so that $I_3 = 0\ A$. Consequently, $I_1 = I_2$ and the ratio (6) becomes:

$$\exp\left(-\frac{eU_3}{kT_e}\right) = 1 + \exp\left(-\frac{eU_1}{kT_e}\right) \tag{9}$$

In which the U_1 is applied externally from a *d.c.* power supply and U_3 is measured by voltmeter in the circuit, which can be directly converted into electron temperature. The T_e value is measured for different U_1. Discuss the errors.

Questions: i) how the system can be used for non stationary plasmas?

ii) get the formula for plasma density?

General remarks:

i) taking into account the assumption made in the model of the TP which are the main limitation of the method?

ii) Can you indicate other limitations?

References

1. J.D.Ewift and M.J.R.Shwar, Electrical Probe for Plasma Diagnostics, ILLFE – Book (1970)
2. I.L.Shohet, The Plasma State, Academic Press (1971)
3. F.F. Chen, Introduction to Plasma Physics, Plenum Press, N.Y., London, (1974)
4. R. Limpaecher and K.R.Mackenzie, Rev.Sci.Instrum., **44** (1982) 726
5. S.I.Chen and T.Sankinguchi. J.Appl.Phys., **36** (1965) 2363

PRACTICUM 6

Measuring of plasma potential with an emissive probe

C. Costin

Purpose

The purpose of this practical work is the direct measurement of plasma potential using an emissive probe.

Theoretical background

An emissive probe is an electrostatic probe heated to electron emission. For a given temperature of the probe, the thermal emission of electrons from the probe into the plasma depends only on the relative voltage between the local plasma potential and the probe bias. It does not depend on other plasma parameters (density, electron temperature, etc). That makes the emissive probe a tool for direct measurement of plasma potential.

Such a probe usually consists of a short wire loop made of tungsten (Fig.1a), which is externally heated by an electric current until electrons are emitted from the surface of the metal, with a current density j_{em} according to Richardson's law:

$$j_{em} = AT^2 \exp\left(-\frac{eW}{k_B T}\right),$$

where A is Richardson constant which depends on the material, T is the temperature of the emitting metal, W is the work function of the metal, e is the elementary charge (1.6×10^{-19} C) and k_B the Boltzmann constant (1.38×10^{-23} J/K). The probe has to be made of a metal with a very high melting point so that it can be heated to high temperature; therefore tungsten is one reliable candidate.

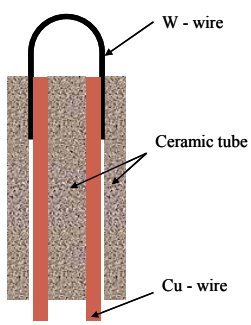

Fig.1a. Schematic of an emissive probe

Fig.1b. Photo of an emissive probe

When the probe is not heated the emissive probe acts like a cold one, having similar current-voltage (I-V) characteristic. When starting to heat the probe it emits electrons. The thermal electron emission current can only flow from the probe towards the plasma as long as the potential of the probe is below the plasma potential. A current of electrons flowing from the probe towards the plasma is equivalent with an ion current flowing from the plasma towards the probe. The two currents add each other resulting thus an increased "ion saturation current" in the I-V characteristic. More the probe is heated, the higher is the "ion saturation current" (Fig.2).

Knowing the relation between the floating potential of the probe (the potential corresponding to a zero current flowing through the probe) and the plasma potential:

$$V_f = V_p - \frac{k_B T_e}{e} \ln\left(\frac{j_{0e}}{j_{0i}}\right),$$

it can be noticed that the increase of the "ion saturation current" j_{0i} makes the floating potential V_f to approach to the plasma potential V_p, the latter two becoming equal when $j_{0i} = j_{0e}$.

When the probe voltage becomes more positive than the plasma potential V_p the thermal emitted electrons are reflected by the plasma back to the probe and no emission current can be detected anymore. The electron current coming from the plasma will be detected as usual.

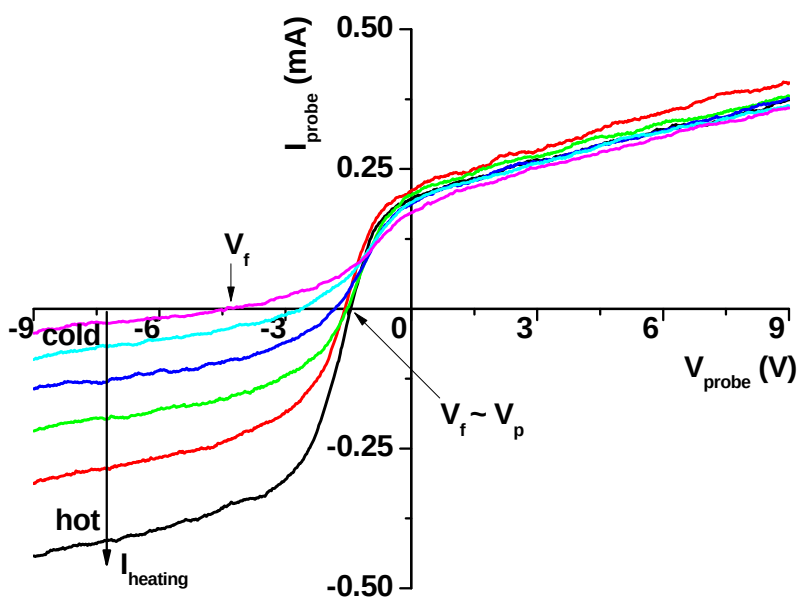

Fig.2. Typical I-V characteristics of an emissive probe

Thus, an emissive probes can be used to directly determine the plasma potential V_p by strongly heating the probe and measuring its floating potential. In practice, as seen in Fig.2, this floating potential is not exactly the plasma potential but it can be considered a good approximation of it. Since the emissive probe draws no current (when floating) it perturbs the plasma much less than the cold probe drawing electron saturation current.

Experimental set-up

The emissive probe is placed in laboratory generated plasma with the purpose of measuring the local plasma potential. Probe's circuit is schematically shown in Fig.3. An external power supply or battery is connected to the probe, generating a high current (of the order of few A) that heats the probe until thermal electron emission (the wire becomes incandescent). The entire circuit has to be floating with respect to the ground or any other electrodes. The voltmeter measures the floating potential of the probe.

It has to be mentioned that when heating the probe a voltage drop of a few V appears across it. This will influence the voltage measured by the voltmeter, depending on where the voltmeter is connected with respect to the loop wire. Different voltage will be measured if the voltmeter is connected in the position 1 or 2 (see Fig.3). In order to avoid this effect, an additional circuit made of two identical resistors can be connected in parallel with the probe. The same voltage drops on the two resistors and on the loop wire, and thus the potential measured in the position 3 is the same as the potential of the midpoint of the loop (point 4).

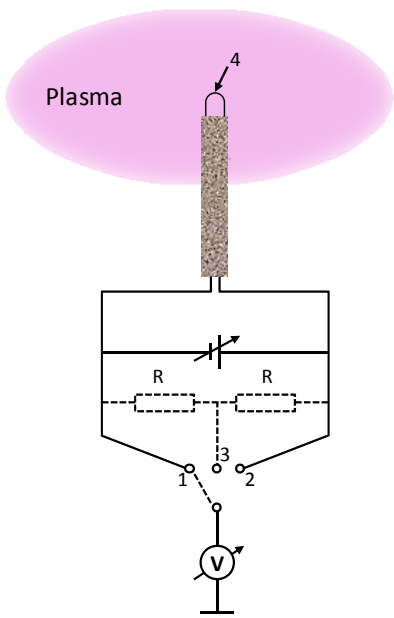

Fig.3. Emissive probe's circuit

If the interest is to draw the current-voltage characteristic of the emissive probe, the voltmeter in Fig.3 has to be replaced by the measuring circuit described in Annex 2.

Suggestions for practicum

1. Manufacture your own emissive probe head. Materials needed: ceramic tube, tungsten wire, copper wire.

2. Draw current-voltage characteristics of the emissive probe having the heating current as parameter. Plot the variation of the floating potential with respect to the heating current. Compare the floating potential of the emissive probe with the plasma potential as it is obtained from the Langmuir probe theory. Decide the optimum heating current of the emissive probe to be used for direct measurements of the plasma potential.

3. Measure directly the local plasma potential in laboratory generated plasma. Determine the local electric field in the plasma form the spatial variation of the plasma potential.

PRACTICUM 7

Determination of ion velocity distribution function by a retarding field analyzer

L. Sirghi

The Retarding Field Analyzer (RFA) allows measurements of the kinetic energy distribution function of charged plasma particles. Usually, the device is used to analyze the kinetic energy or velocity distribution functions of ions, which is not possible to do with Langmuir probes. In principle, the idea of RFA consists in using of a biased grid placed between the plasma and a planar Langmuir probe, which collect the charged particles separated by the grid (Fig. 1a). To analyze the ions, the grid is biased at a negative potential to reject the plasma electrons. Analysis of ion energy by Langmuir probes in plasmas is impossible because in the ion repelling region the probe collects the electron saturation current, which is much larger than the ion current. Therefore, an ion separation grid is placed between the plasma and the ion collecting electrode in order to reject the electrons back into the plasma. Figure 2 presents I-V characteristics obtained by a RFA with a single grid biased at -50V, -70V and -100 V, respectively, in the multipolar magnetically confined plasma. Intentionally, this plot considers the ion collecting current negative and the electron collecting current positive as for the Langmuir probe I-V characteristics. The I-V characteristic obtained at V_g = -50 V resembles the I-V characteristic of a single Langmuir probe with a strong, but not complete, attenuation of the collected electron current. The attenuation of the electron current is enhanced by the increase (in absolute value) of the negative biasing potential of the grid, a total rejection of electrons being obtained at V_g = -100 V.

1. Design and working principle of three grid retarding filed analyzer

However, using a RFA with a single grid has some problems that impede a correct determination of ion kinetic energy distribution. Firstly, the negatively biased grid is hardly rejecting all the plasma electrons in the case of plasmas with the Debye length smaller than the holes of the grid because the plasma screens the electric field of the grid and can penetrate into the space between the grid and the current collecting probe. This is why the total rejection of electrons in the analyzer with a single grid is achieved only at large values of V_g (Fig. 2). To overcome, this problem the RFAs use a collimator to extract a small amount of plasma particles and a plasma separation grid that is usually grounded to establish a reference

for the electrostatic energy (Fig. 1b). The density of plasma after it diffuses in the collimator space and separation grid is much smaller than the bulk plasma outside the RFA and this yields a much larger Debye length at the electron separation grid G_2. Indeed, the Debye length is computed by

$$\lambda_D = \sqrt{\frac{\varepsilon_0 k_B T_e}{e^2 \cdot n}} = 7400mm \cdot \sqrt{\frac{k_B T_e [eV]}{n[cm^{-3}]}}, \quad (1)$$

where $k_B T_e$ is the electron temperature in eV, e, the elementary electric charge, ε_0, the vacuum dielectric permitivity, and n, the plasma density. Typical values of $k_B T_e$ and n for multipolar magnetically confined plasma device are 0.6 eV and 6×10^9 cm^{-3}, respectively, which yeld a Debye length of 74 μm. This can be smaller than the dimension of grid holes (typically 150 μm). A decrease of plasma density intro the collimator to about one tenth of its bulk value leads to an increase of Debye length with a factor of 3.

A second problem of RFA with a single grid is caused by secondary electron emission of RFA electrodes. The ion collecting probe (the plate of the RFA) is heated by energetic ions (especially at large negative values of its biasing potential, V_c) and this may result in secondary emission of electrons. This secondary emission current is "seen" on the RFA I-V characteristic as an increase of the ion collected current, and this can result in a large distortion of the determined ion energy distribution function. This effect is visible in Fig. 2, which at large negative values of V_p shows a larger collected ion current at V_g = -100V than at V_g = -70V. The solution of this problem consist in using a secondary emission suppression grid biased negatively at few volts with respect of V_p in order to reject the electrons emitted through secondary emission by the plate of the analyzer. Therefore, the classical RFA used by researchers to measure the ion kinetic energy distribution is a device with three grids as represented in Fig. 1b. The spatial distribution of the space potential, V_s, in the RFA in the ideal case of no screening of spatial charges is also represented. This latter condition is fulfilled when the current density of electric charges collected by the RFA electrodes is much smaller than the Child-Langmuir current density:

$$j_{CL} = \frac{4}{9}\varepsilon_0 \cdot \sqrt{\frac{2e}{m_i}} \cdot \frac{V^{3/2}}{d^2}, \quad (2)$$

where V is the electrode biasing potential, d, the thickness of space charge sheath, and m_i, the ion mass. This imposes restrictions on the values of biasing potential of RFA electrodes and distance between them (not very high value of V and very small values of d).

While the collector potential V_c is lower than the plasma potential V_p, the collector (C) collects all the positive ions entering into the device. When V_c is made negative ($V_c < V_p$) the ions with the kinetic energy $E_c < e(V_p\text{-}V_c)$ are rejected and not collected by the plate. This leads to sudden decrease of the ion current, I_c. The $I_c(V_c)$ characteristic gives the information on the ion kinetic energy distribution.

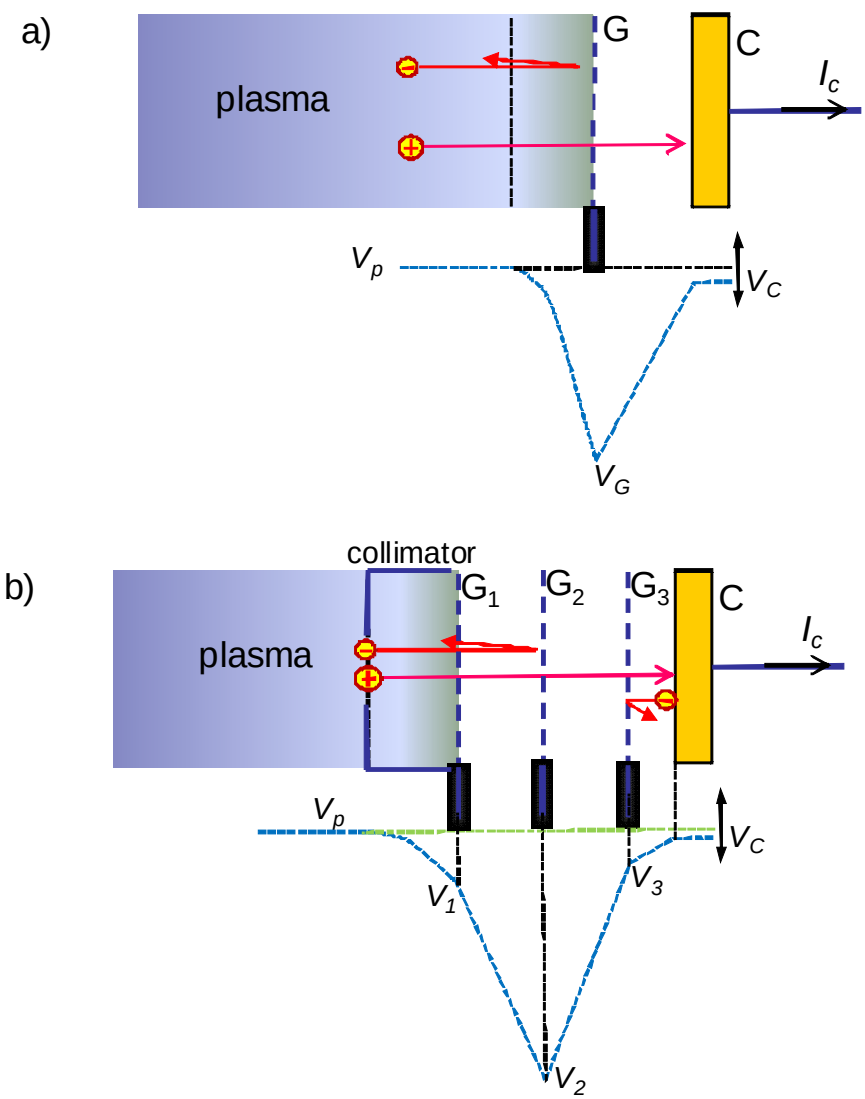

Fig. 1 Sketches of one-grid analyzer illustrating the principle of the ion kinetic energy distribution measurements (a) and the three-grid analyzer (b). The distribution of spatial potential in nearby plasma (where a spatial sheath of positive spatial charge is formed) and inside the device is also illustrated. While the collector potential Vc is lower than the plasma potential Vp, the collector (C) collects all the positive ions entering into the device. When Vc is made negative (Vc < Vp) the ions with the kinetic energy Ec < e(Vp-Vc) are rejected and not collected by the plate. This leads to sudden decrease of the ion current, Ic. The Ic(Vc) characteristic gives the information on the ion kinetic energy distribution.

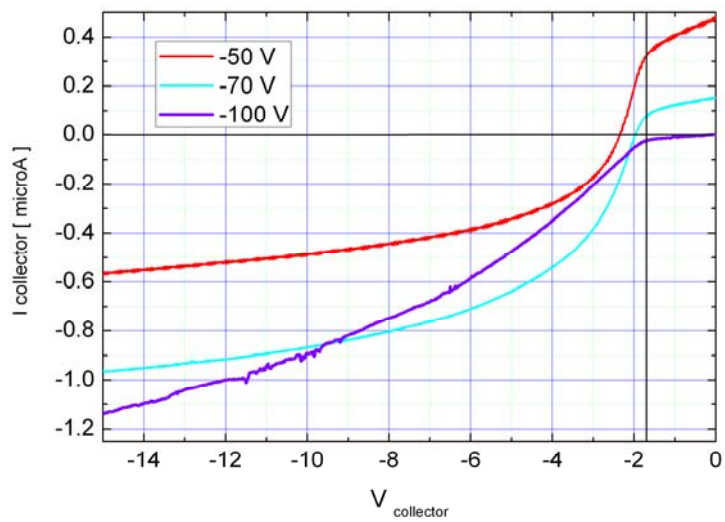

Fig. 3 I-V characteristics obtained by a RFA with a single grid biased at -50V, -70V and -100 V, respectively, in the multipolar magnetically confined plasma. The I-V characteristic obtained at V_g = -50 resembles the I-V characteristic of a single Langmuir probe with a large attenuation of the collected electron current. The attenuation of the electron current is enhanced by the increase (in absolute value) of the negatively biasing potential of the grid, a total rejection of electrons being obtained at V_g = -100 V.

2. Theoretical background

The ion current collected by the RFA collector, I_c, is:

$$I_c = \theta \cdot e \cdot A \cdot \int_{v\min}^{\infty} v_x \cdot f_i(v_x) \cdot dv_x \,, \tag{3}$$

where e is the ion electrical charge, A, the ion collecting area, θ, the total transparency of the grids, $f_i(v_x)$, the ion velocity distribution function along the RFA axis x, and v_{min} is the minimum velocity along the x axis of ions that reach the collector. This minimum velocity corresponds to the minimum kinetic energy of ions:

$$E_{i\min} = \frac{m_i \cdot v_{\min}^2}{2} = e(V_c - V_p)\,. \tag{4}$$

The eq. (3) leads straightforwardly to the fallowing equation for $f_i(v)$:

$$f_i(v_x)\Big|_{v=\sqrt{2e(V_c-V_p)/m_i}} = -\frac{m_i}{e^2} \cdot \frac{1}{\theta \cdot A} \cdot \frac{dI_c}{dV_c} \quad , \tag{5}$$

where dI_c/dV_c is the first derivative of $I_c(V_c)$.

For a Maxwellian ion distribution function,

$$f_i(v_x) = n_i \cdot \left(\frac{m_i}{2\pi T_i}\right)^{1/2} \cdot \exp\left(-\frac{m_i v_x^2}{2T_i}\right), \tag{6}$$

the equation (3) yields the fallowing expression of I_c:

$$I_c = e \cdot n \cdot \theta \cdot A \cdot \left(\frac{T_i}{2\pi \cdot m_i}\right)^{1/2} \cdot \exp\left(-\frac{eV}{T_i}\right), \tag{7}$$

where V is the ion energy retarding potential ($V = V_c - V_p$).

Therefore, in the ion energy retarding biasing potential ($V_c > V_p$), the derivative dI_c/dV_c is:

$$\frac{dI_c}{dV_c} = -e^2 \cdot n \cdot \theta \cdot A \cdot \left(\frac{1}{2\pi \cdot m_i \cdot T_i}\right)^{1/2} \cdot \exp\left(-\frac{eV}{T_i}\right) \tag{8}$$

The eq. (8) gives $f_i(v_x)$ for $v_x > 0$ in the ion retarding potential of the I-V characteristic (V > 0). Figure 4 presents schematically the functions $I_c(V_c)$ and dI_c/dV_c given by eqs. (7) and (8) for a Maxwellian ion distribution function with T_i = 0.1 eV. At V= 0, the dI_c/dV_c has a discontinuity, dI_c/dV_c being 0 for $V < 0$ (where I_c is constant and equal to the ion saturation current intensity). The full width at half maximum of the peak value (FWHM) of dI_c/dV_c is $\Delta V = T_i \cdot ln2/e = 0.69 \cdot T_i/e$, which estimates the ion temperature as $T_i = 1.44 \cdot e \cdot \Delta V$.

However, the RFA is seldom picking up a drifted ion energy distribution due to the positive charge sheath between the plasma separation grid and the bulk plasma (see Fig. 1 for a schematic of space potential distribution in RFA). For a drifted Maxwellian ion energy distribution function with temperature T_i and drifting velocity v_i, the I-V characteristic of RFA is given by the fallowing equation [x]:

$$I_c(V) = \frac{e}{\sqrt{2\pi\, m_i}} \cdot n \cdot \theta \cdot A \cdot \left[\sqrt{T_i} \cdot \exp\left(-\frac{\left(\sqrt{eV} - \sqrt{E_i}\right)^2}{T_i}\right) + \sqrt{\pi \cdot E_i} \cdot erf\left(\frac{\sqrt{eV} - \sqrt{E_i}}{\sqrt{T_i}}\right)\right] \tag{9}$$

where $E_i = m_i v_i^2/2$ is the kinetic energy of ions corresponding to the drifting velocity v_i.

In this case:

$$\frac{dI_c}{dV_c} = -e^2 \cdot n \cdot \theta \cdot A \cdot \left(\frac{1}{2\pi \cdot m_i \cdot T_i}\right)^{1/2} \cdot \exp\left(-\frac{\left(\sqrt{eV} - \sqrt{E_i}\right)^2}{T_i}\right), \tag{10}$$

And the FWHM of dI_c/dV_c peak centered at $V_c = V_p + E_i/e$ (see Fig. 4) is $\Delta V = \left(4 \cdot \sqrt{T_i \cdot E_i}\right)/e$.

Note that in this case, ΔV does not give direct information on T_i. Beacouse, usually, $E_i >> T_i$, ΔV is enlarged very much by the drift. If v_i is the Bohm velocity, $E_i = T_e$ and

$\Delta V = \left(4 \cdot \sqrt{T_i \cdot T_e}\right)/e$. In this case knowledge of T_e is required in order to find the value of T_i. For example, for a Maxwellian ion distribution with temperature T_i = 0.1 eV, ΔV is 0.069 V, while for a drifting Maxwellian with Bohm velocity with T_i = 0.1 eV and T_e = 1 V, ΔV = 1.26 V. Figure 4 presents the theoretical I-V characteristics of a RFA picking up ions with Maxwellin and drifted Maxwellian distributions, respectively.

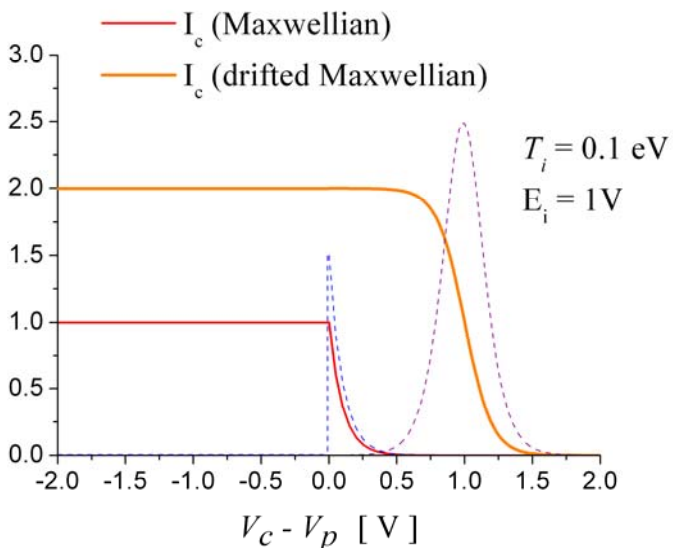

Fig. 4 Theoretical I-V characteristics and their derivatives obtained for a Maxwellian ion velocity distribution function (T_i = 0.1 eV) and for a drifted Maxwellian ion velocity distribution function (T_i = 0.1 eV and E_i = 1 V).

Experiment

Figure 5 presents a LabView panel with plots of $I_c(V_c)$ characteristic and its first derivative (dI_c/dV_c) obtained with a three-grid RFA in the multipolar magnetically confined plasma device. Details on the construction of RFA are presented in the practicum documentation. The plasma separation grid was floating while the electron biasing grid was biased at -70V. The biasing potential of the collector was swept 60 times between 0 and -15 V with steps dV = 0.015V and the corresponding I_c data points were acquires 60 times for each biasing potential value. The I_c values were averaged to improve the signal-to-noise ratio. The analyzer has been installed on the axis of the multipolar magnetically confined plasma device at a distance of 10 cm from the end flange (see the practicum documentation). The data has been collected in argon plasma at pressure of $4 \cdot 10^{-4}$ mbar, at a discharge current intensity of 100 mA and discharge voltage of 70 V. A peak in dI_c/V_c is observed near the plasma potential, V_p. The full width at half maximum of the peak value (FWHM) was determined to about 0.85 eV.

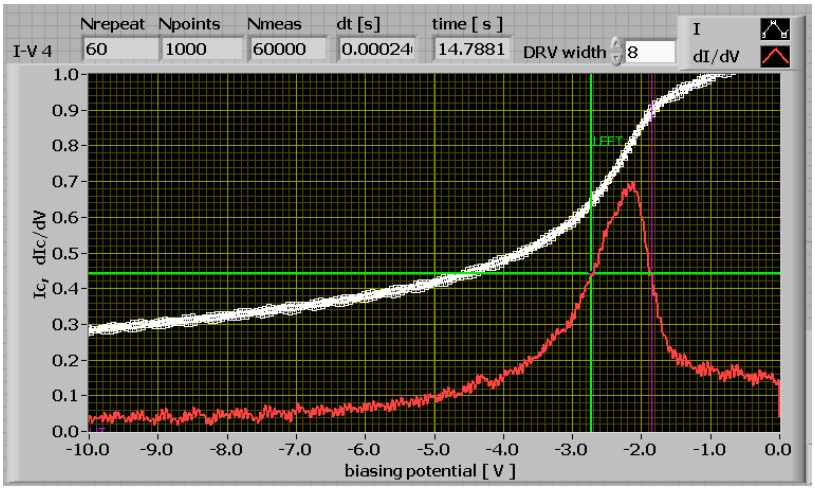

Fig. 5 LabView front panel with an I_c-V_c characteristic and its first derivative, dI_c/dV_c, obtained in the multipolar magnetically confined plasma (argon at 4 x 10^{-4} mbar, ad U_d = 70 V and I_d = 100 mA) with a three-grid RFA. The electron separation grid has been biased at -70V and V_c was swept between 0V and -15V is 1000 steps.

The shape of I-V characteristic and the FWHM value of its derivative indicate that the RFA is picking up ions accelerated in a plasma sheath at Bohm speed. A value of 1.3 eV can be considered for the drifting kinetic energy on the basis of electron temperature measurements (see Practicum 1). This determines a value of 0.04 eV for T_i.

Determination of ion concentration is possible if the total transparency factor of the grids, β, is known.

References

[x] N. Hershkowitz, Plasma Diagnostics, Vol 1(Ed. Orlando Auciello and Daniel L. Flamm, Academic Press Inc. Boston, San Diego 1989), Chap. 3, p. 123.

DOCUMENTATION 2

Data acquisition system for automatic acquisition of electrical probe I-V characteristics

L. Sirghi

Basically, the data acquisition system used for acquisition of probe I-V characteristics consists of an electrical power supply used for probe biasing and a current intensity instrument connected as in Fig. 1. In order to perform the data acquisition automatically and to save the I-V data digitally on a PC, these two devices should be controlled by a computer via digital-to-analog (DAC) and analog-to-digital (ADC) converters. The number of data points (measurements) and timing of the I-V acquisition is defined by user according to the performances of PC, DAC, and ADC. The sweeping the probe biasing potential, V_b, between certain user defined values (V_{min} and V_{max}) is done in N steps, at each step V_b being increased with $\Delta V = (V_{max}-V_{min})/(N-1)$. The value of ΔV is important because it defines the voltage resolution of the measurement. The measurement of probe current, I, at certain value of the biasing voltage can be repeated of N_{repeat} times and averaged in order to increase the signal to noise ratio.

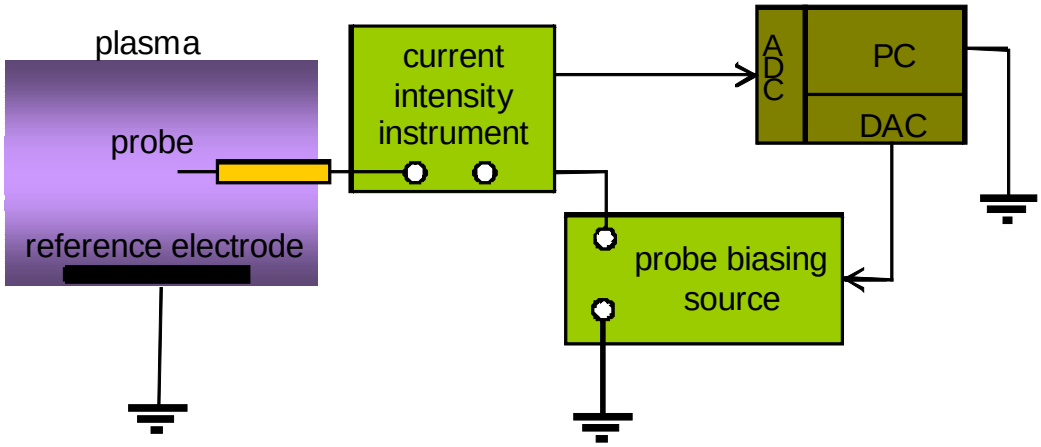

Fig. 1 The block diagram of a data acquisition system used in automatic acquisition of I-V probe characteristics.

There are some common problems related to the use of the digital data acquisition system for automatic acquisition of Langmuir probe I-V characteristics as it fallows:

1) As it is shown in Fig. 1, the probe biasing circuit should contain a reference electrode that should have a good electrical contact with plasma. The area of the electrode should be much larger than the active area of the probe so that the ion saturation current of the reference electrode to be larger than the electron saturation current of the probe;

2) The probe biasing power supply should generate the biasing voltage values around plasma potential V_p in a sufficiently large interval (ex. $V_{min} = V_p$-10V, $V_{max} = V_p$+10 V). This can be a problem if V_p is very large. Fortunately, V_p for multi polar magnetically confined plasma has values around 0 V.

3) The current intensity instrument should be floating. In the case it is not, the V_b, which is the bias voltage at the instrument input terminals, can not exceed the certain limited values (usually ± 15 V).

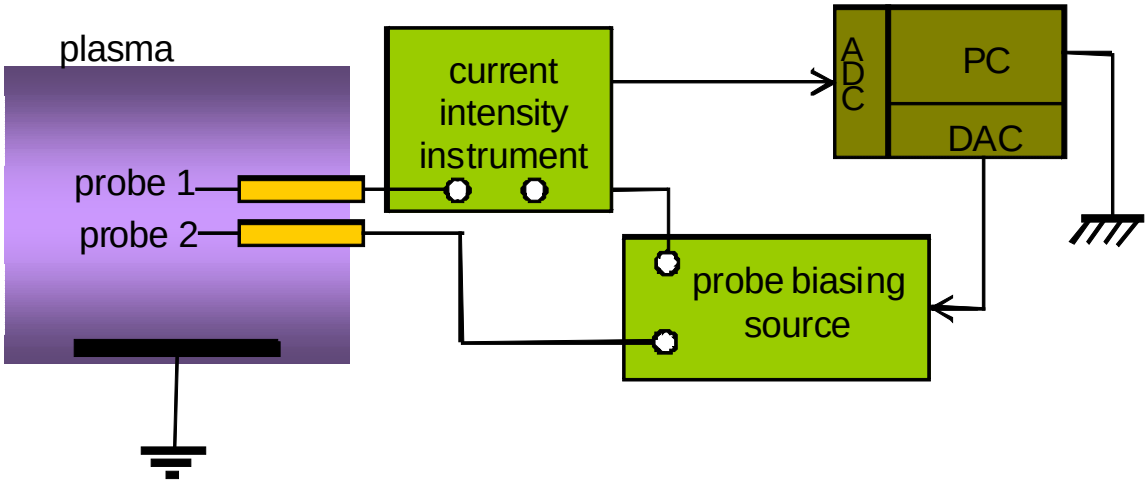

Fig. 2 The block diagram of a data acquisition system used in automatic acquisition of I-V characteristics for a double probe. The measuring circuit and the double probe should be floating with respect to plasma. Therefore the plasma system and the measuring system should not have a common ground.

4) The PC, biasing power source and plasma device (reference electrode) should have a common ground. This means that this data acquisition system can not be used for acquisition of double probe I-V characteristics, because in this case the measuring circuit should be floating with respect to plasma (Fig. 2).

5) The voltage generated by the electrical power supply (biasing source) can be different of the biasing voltage due to the finite internal electrical resistance (impedance) of the current intensity measuring instrument.

The data acquisition system used in our laboratory overcomes all these problems by using a Source Meter Instrument (SMI) (2612A from Keithley) connected to a PC (Fig. 3). The SMI can generate a biasing voltage in the range ± 200V and measure in the same time, or with a user-defined delay time, the probe current intensity. The instrument has an internal processor that controls the data acquisition according to the user settings. Moreover, the current source of the SMI can be connected in the probe biasing circuit in either single ended or floating configurations, which means that the SMU can be used for either single or double probe measurements.

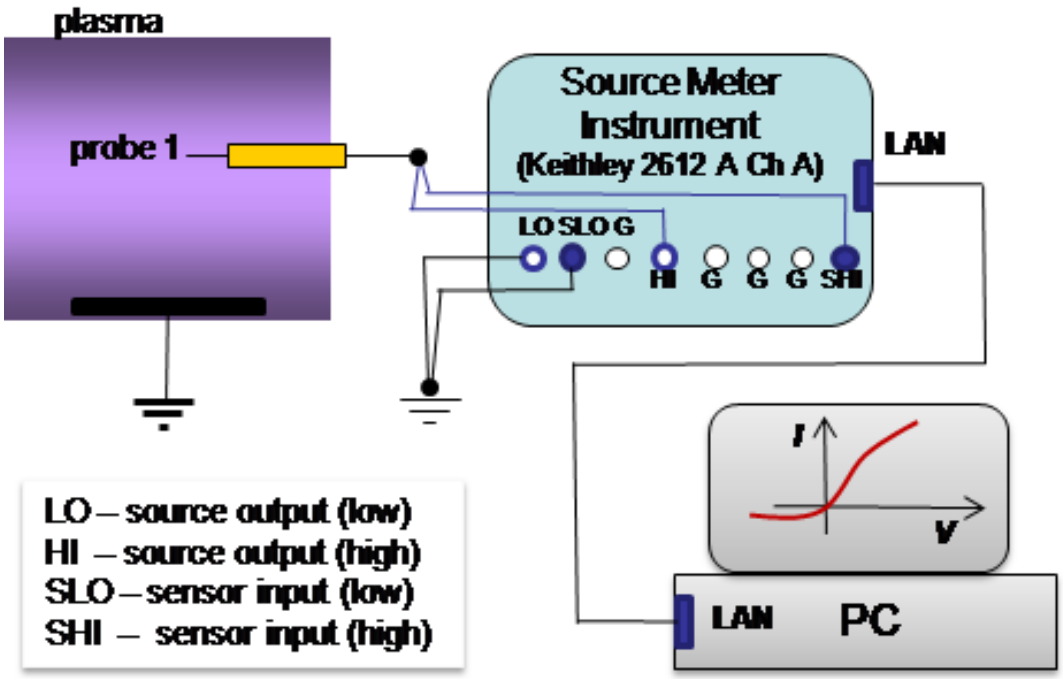

Fig. 3 Block diagram and electrical connection of automatic data acquisition system used for acquisition of probe I-V characteristics. The system uses a source meter instrument (SMI) connected to a PC through a LAN connection. The source output and sensor input terminals are connected to the probe in remote sensing connection.

Figure 3 presents a sketch of the probe biasing circuit that uses the SMI Keithley 2612A connected to a PC through a LAN connection. The voltage source and current reading instrument of the SMI is connected to the probe in the remote sensing configuration on the channel A of the SMI. The LAN connection of the SMI to the PCI is done via Internet Explorer by using the IP address of the instrument (169.254.0.1 in the case shown in Fig. 4). Following this, the Internet Explorer accesses the Home Page of the SMI (Fig. 5).

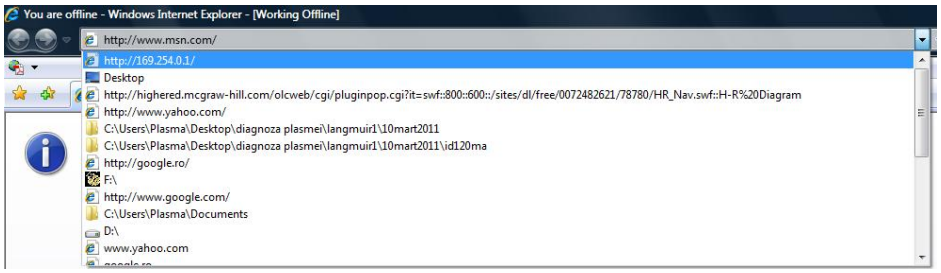

Fig. 4 Connection of the SMI to PC via Windows Internet Explorer

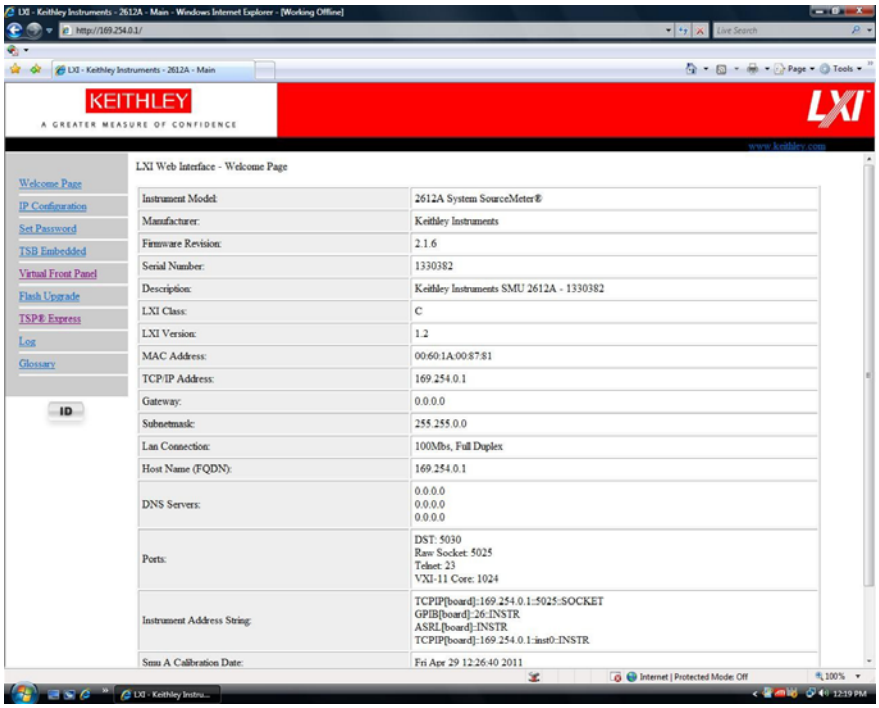

Fig. 5. Example of the SMI home page.

The probe I-V characteristic acquisition can be controlled by the TSP Express software program, which is launched from the SMI home page. Figure 6 presents an example of quick start of Single SMU sweeps measurements program used for automatic acquisition of the probe I-V characteristics.

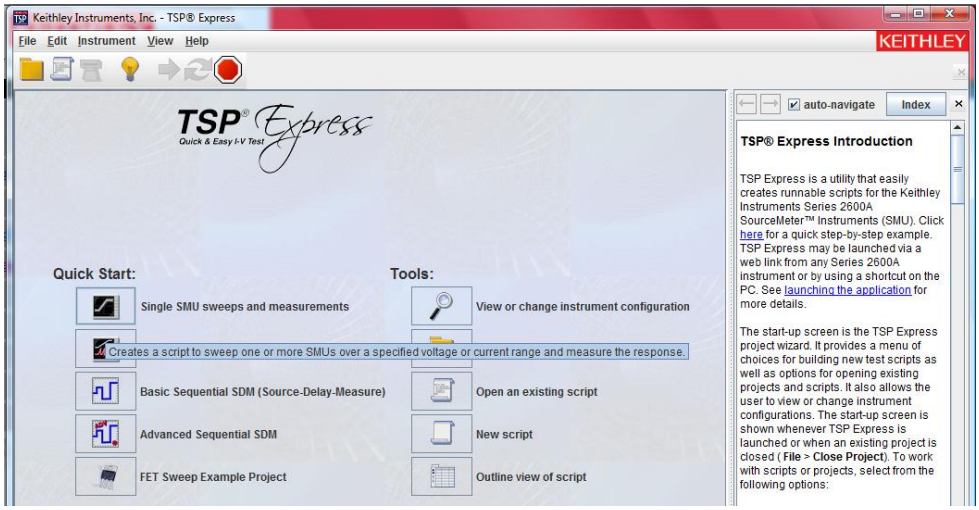

Fig. 6 Launching the Single SMU (source measuring unit) sweeps and measurements

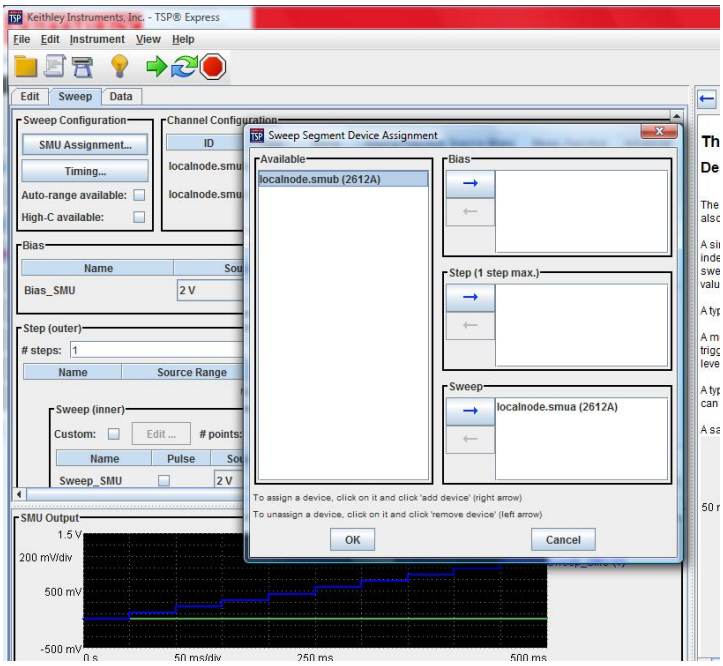

Fig. 7 Assignment of channel A (localnode.smua) for sweeping the biasing voltage of the Langmuir probe. The channel B of the instrument is not used.

The I-V probe data acquisition is controlled by the TSP Express program fallowing the user settings of SMU Assignment, channel configuration, timing, sweep configuration as is illustrated by the Figures 7, 8, 9, and 10.

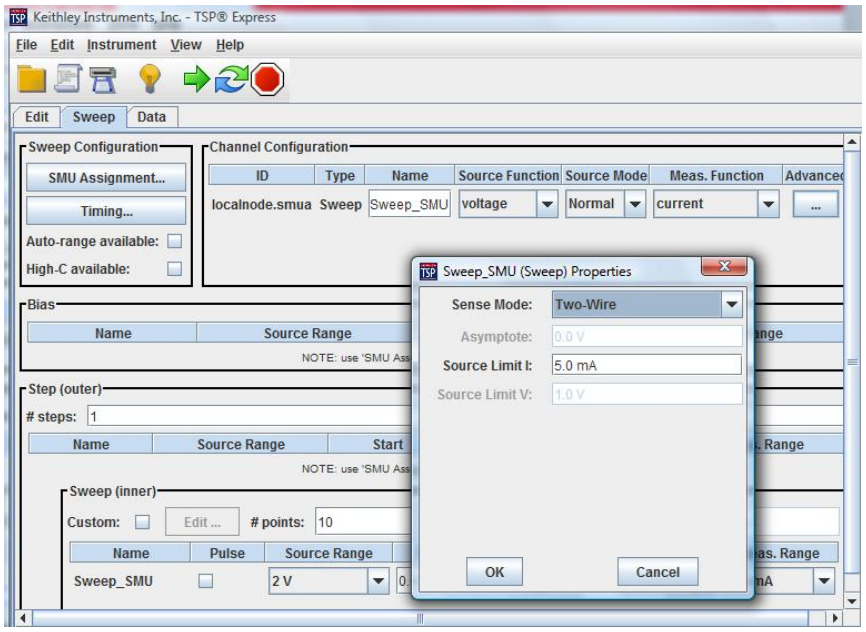

Fig. 8 Setting of the SMU channel configuration (sensing mode and source current intensity limit).

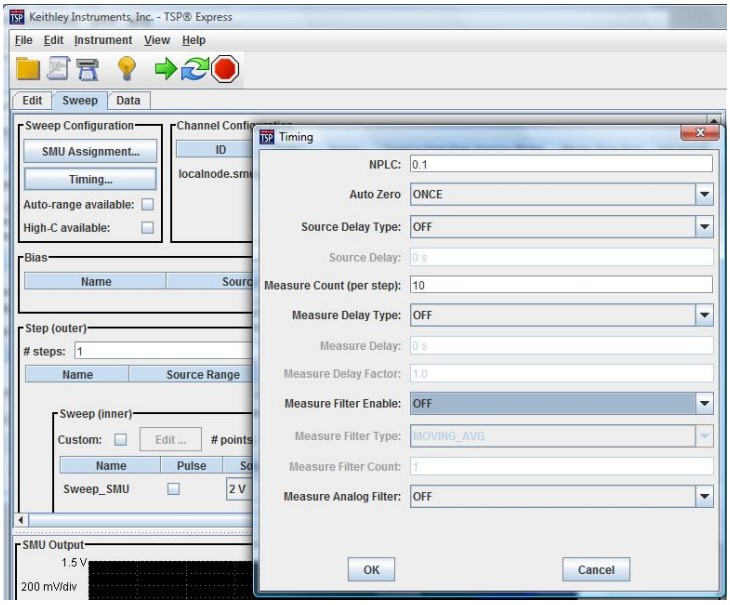

Fig. 9 Setting of the data acquisition timing parameters. To improve the signal to noise ratio, the current intensity readings for each voltage step is set to 10 times. Also, the program allow for setting of a delay time between voltage update and current intensity reading.

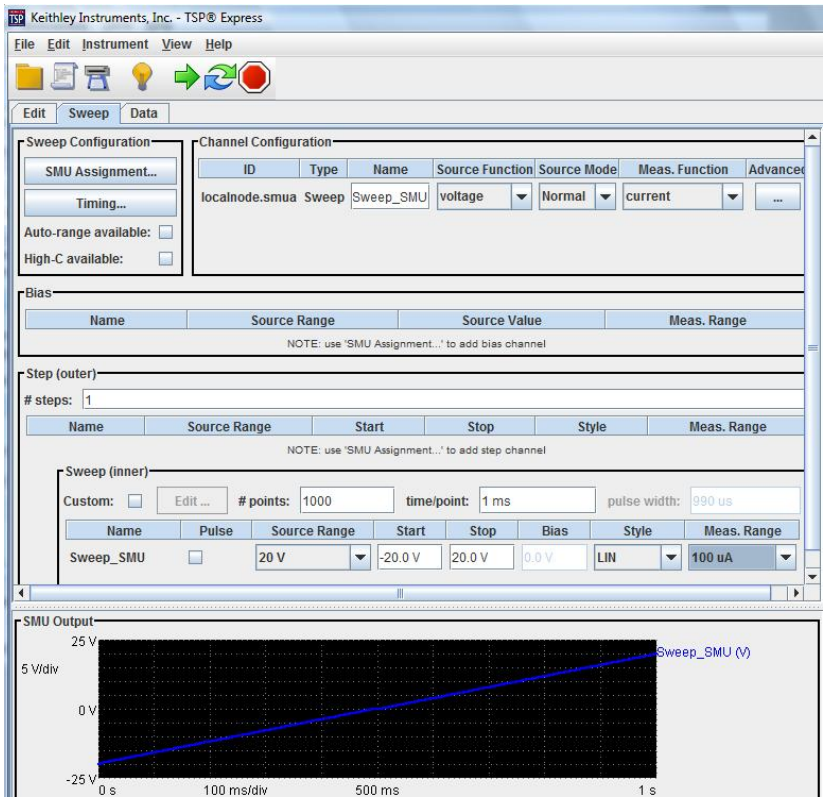

Fig. 10 Example of settings used for sweeping of the probe biasing voltage between -20V and +20V in 1000 steps in 1ms time per step, the scale of the current intensity sensor being 100 µA.

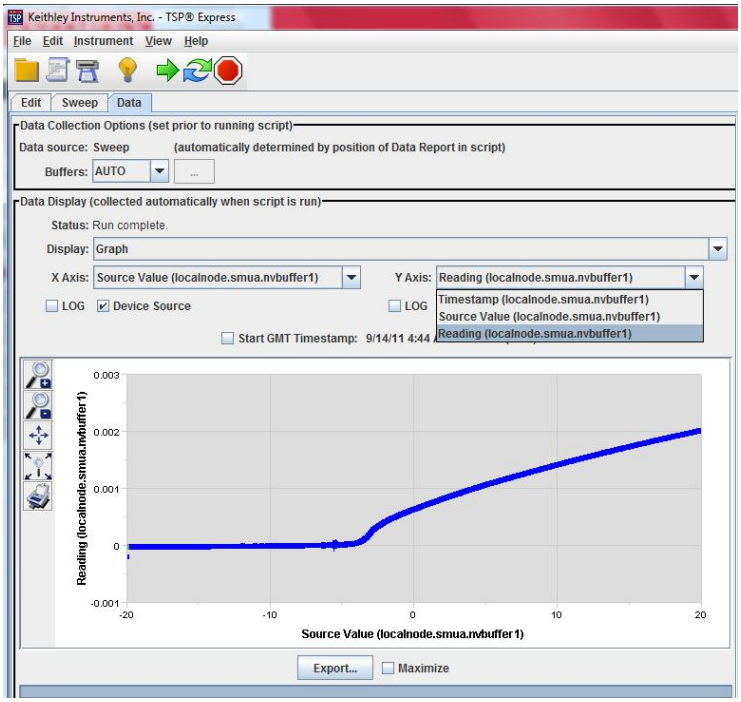

Fig. 11 View of the I-V characteristic as a plot of I as function of V

After the data acquisition parameters being settled, the program can be run to acquire the probe I-V characteristics. The I-V data can be viewed as a plot on a graph (Fig. 11) or as a table (Fig. 12). Finally, the data can be saved as a (coma separated values) CSV type file by pushing the “Export” button. The CVS files with data if the probe I-V characteristics are processed offline by loading them by specialized software in LabView. Figures 13 and 14 presents the front panel and the block diagram of the LabView program used to read the CVS files and to provide the averaged I-V characteristics in the increasing order of the sweeping voltage.

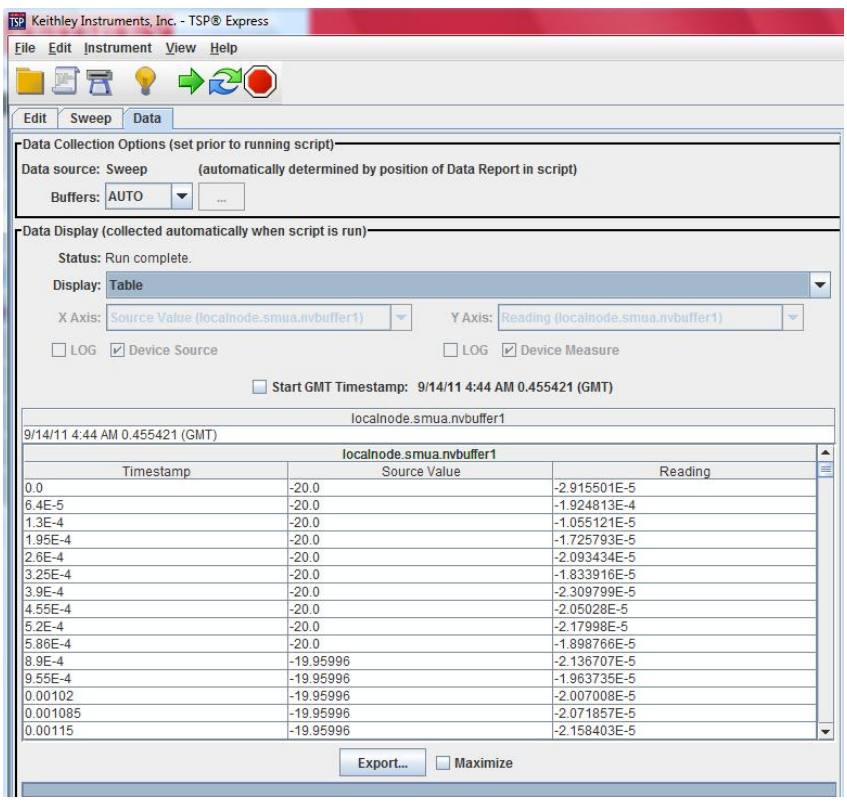

Fig. 12 View of the I-V characteristic data as a table. The button “Export” is used to save the data into a CSV type file.

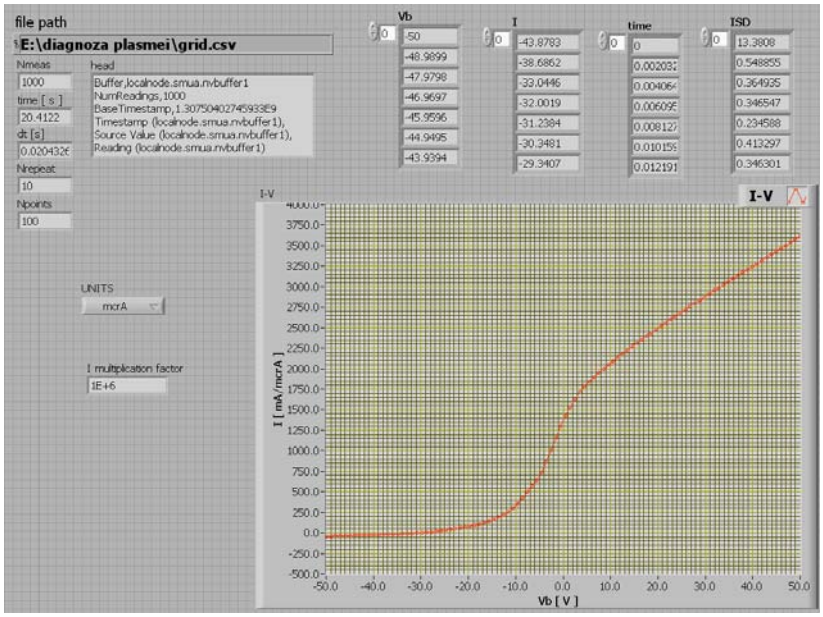

Fig. 2 The front panel of the LabView program that open and read the CSV files with probe I-V characteristic data.

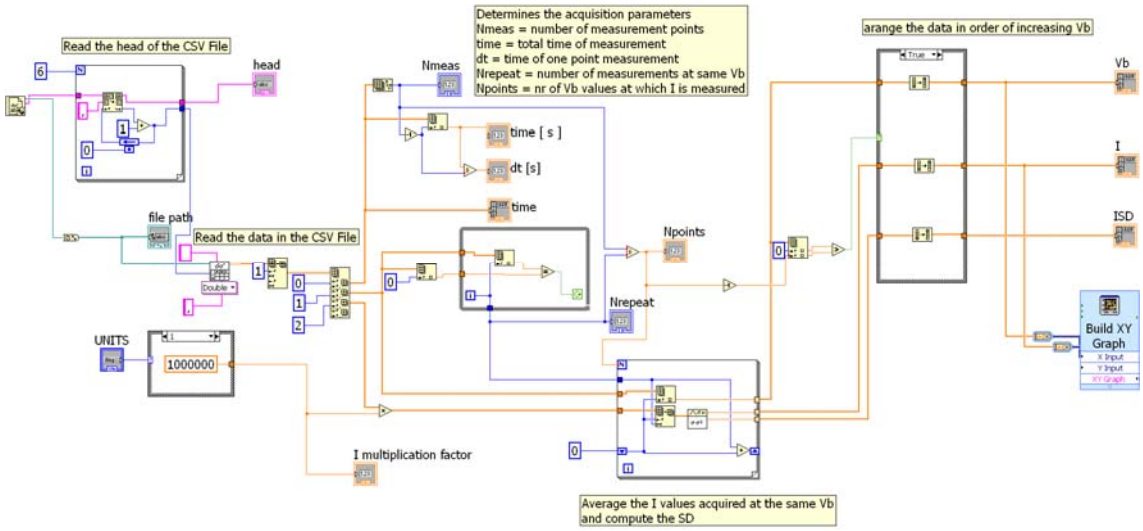

Fig. 2 The block diagram of the LabView program that open and read the CSV files with probe I-V characteristic data.

DOCUMENTATION 2

Multi-polar Magnetically Confined Plasma Diagnostics by Electrical Probes

L. Sirghi

The present documentation gives technique details on construction and usage of:

1. multi-polar magnetically confined plasma device and the vacuum pumping system
2. home-made probes (single, double, triple and emissive probe with direct heating)
3. home-made electrostatic analyzer with tree grids.
4. probe biasing circuit and digital data acquisition of probe I-V characteristics.

1. Construction of the multi-polar magnetically confined plasma device

Figure 1 presents schematically the multi-polar magnetically confined plasma device used in the present practicum. The device uses a large (40 L) discharge chamber connected to a vacuum system and a gas feeding circuit. Inside the chamber there are mounted one or two cathodes and one or two cylindrical anodes with rows of magnets to generate a confining magnetic field near the anode and discharge chamber walls.

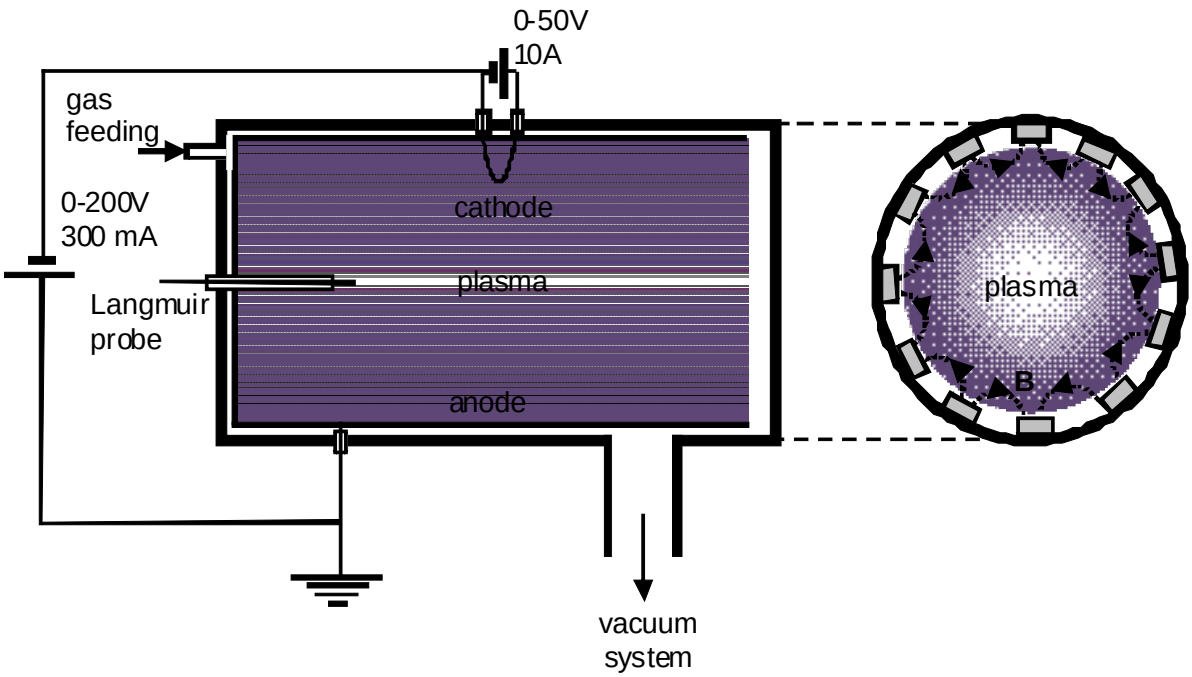

Fig. 1 Sketch of multi-polar magnetically confined plasma device used in the practicum.

The plasma is obtained by maintaining an electrical discharge between the cathode, which is heated to the thermoemission, and the anode, which can be the inner wall of the discharge chamber, in a gas (usually argon) at a pressure ranged between 10^{-4} to 10^{-3} mbar.

The main part of the multi-polar magnetically confined plasma device is the discharge chamber, which is made from stainless steel walls with thickness of about 10 mm. Figure 2 presents a photo of the inside of the dismounted chamber (without lateral flanges, anode and cathode). The upper apertures are used for filament cathode and anode connections, while the bottom aperture is used for connection to the vacuum system. The lateral aperture is used for a visualization window. Figure 2 present a detailed technical sketch of the chamber with all dimensions given in mm.

Fig. 2 Photo of the inside part of the chamber used in the multi-polar magnetically confined plasma device. The upper apertures are used for filament cathode connections, while the bottom aperture is used for connection to the vacuum system. The lateral aperture is used for a visualization window.

The lateral (left and right) openings of the chamber are connected to flanges (which are also represented on the sketch) while the upper openings are used for cathode and anode connections. The bottom opening is connected to the vacuum system. The flanges have many openings used for mounting of the electrical probes and gas feeding system. Figure 3 presents a technical drawing with the view of one end of the discharge chamber, where a flange is mounted to close the chamber. The end has a channel (10 mm in width, 5mm in depth and 320 mm in diameter) for the rubber O-ring used to seal the chamber when the flange is tightly mounted by 8 screws ($\Phi = 9$ mm) and groves (not shown). The rubber O-ring and the channel is visible in the photo shown in Fig 1 and are also represented in the drawings in Figs 2 and 3.

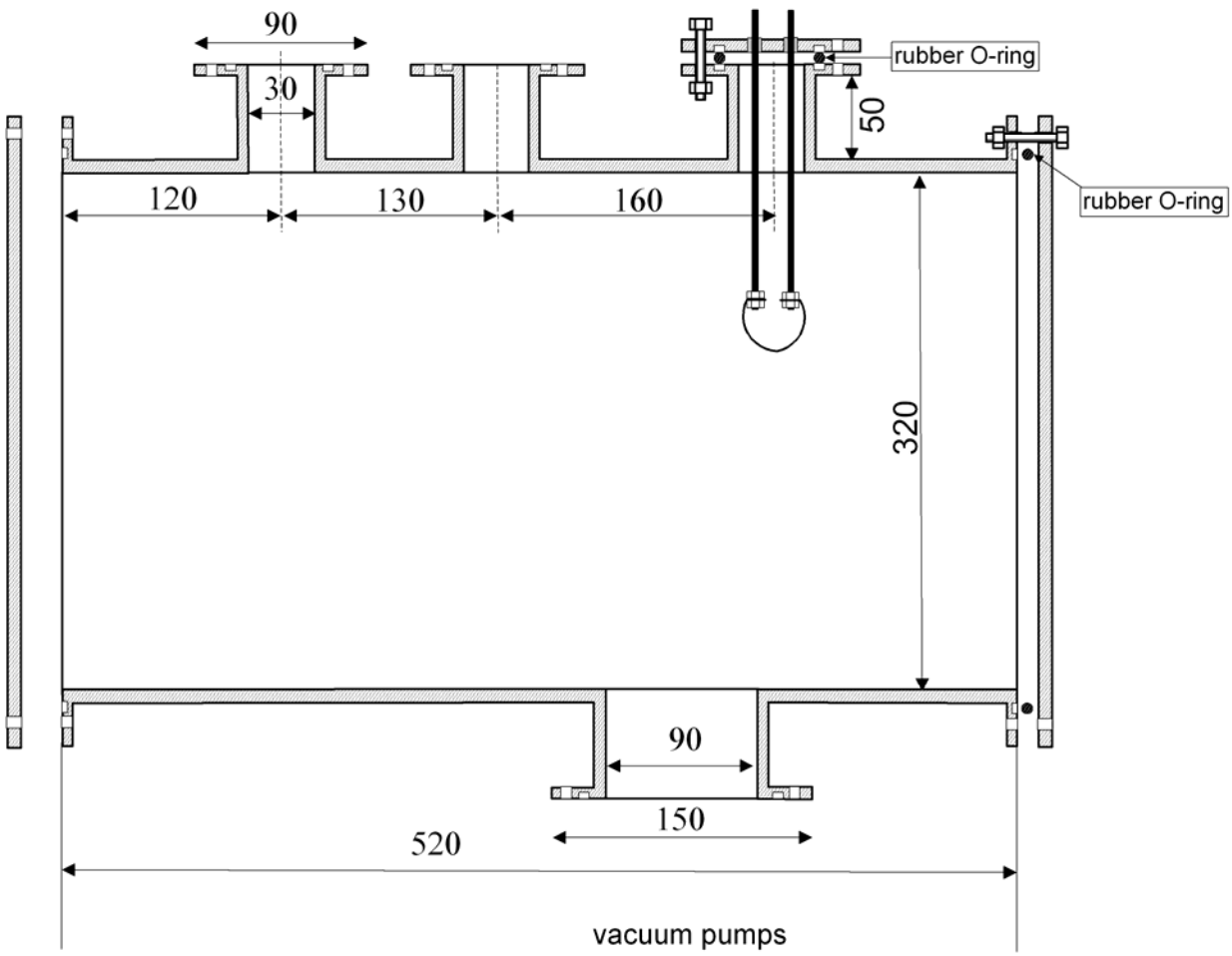

Fig. 3 Technical drawing with the cross section view of the discharge chamber. Al the dimensions are given in mm. The lateral (left and right) openings of the chamber are connected to flanges (which are also represented on the sketch) while the upper openings are used for cathode and anode connections. The bottom opening is connected to the vacuum system. The flanges have many openings (not shown) used for mounting of the electrical probes and gas feeding inlet.

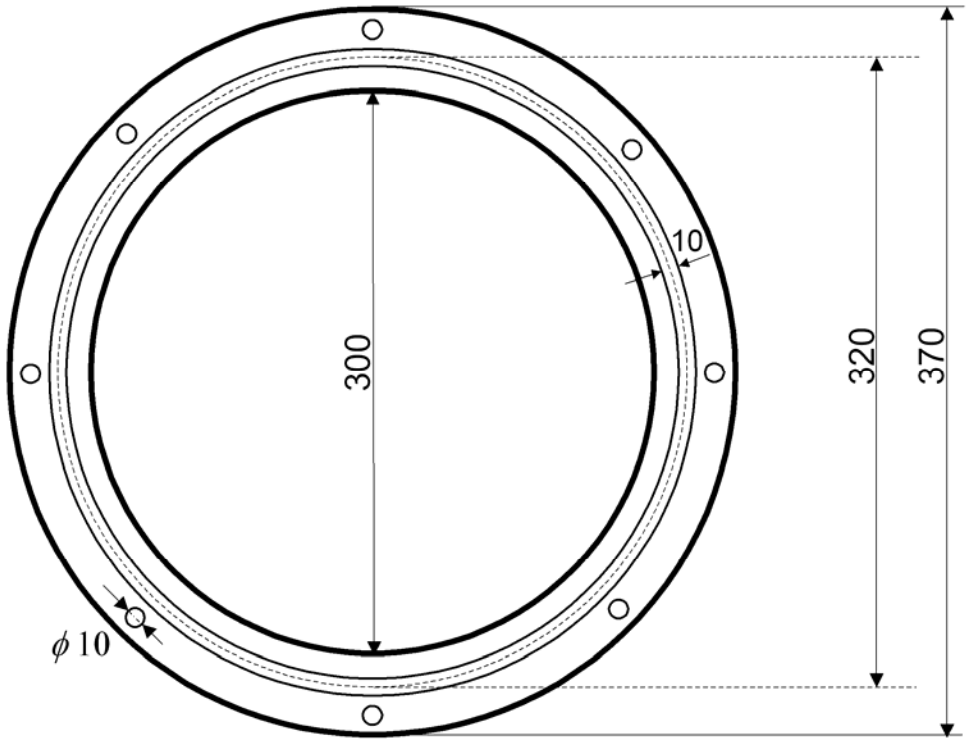

Fig. 4 Technical drawing with the view of one end of the discharge chamber. The chamber end has a channel (320 mm in diameter, 10 mm in width and 5mm in depth) for the rubber O-rings and 8 holes (10 mm in diameter) for mounting of the end flange.

The anode is a cylinder (270 mm in diameter and 250 mm in length) made of stainless steel foil (2 mm in thickness). Figure 4 shows a photo of one cylindrical anode. Rows of magnets are mounted on the inner part of the anode. The multi-polar magnetically confined plasma device in the Plasma Physics Laboratory of Iasi has two anodes with length of 250 mm. One anode is connected electrically to the ground while the other can be connected to a different electrical potential through a dc power supply. This configuration allow for running of two independent plasma sources in the same discharge chamber. However, for simplicity the two anodes are both connected to the ground. The two anodes with the length of 250 mm each can be replaced by one anode with the total length of 500 mm. A technical drawing representing the top view of the cylindrical anode is given in Fig. 5. The rows of magnets (with cross section of 7×10 mm^2 and with magnetic field of 300 Gs at surface) are mounted with alternate polarity with a space of about 30 mm between neighbor rows.

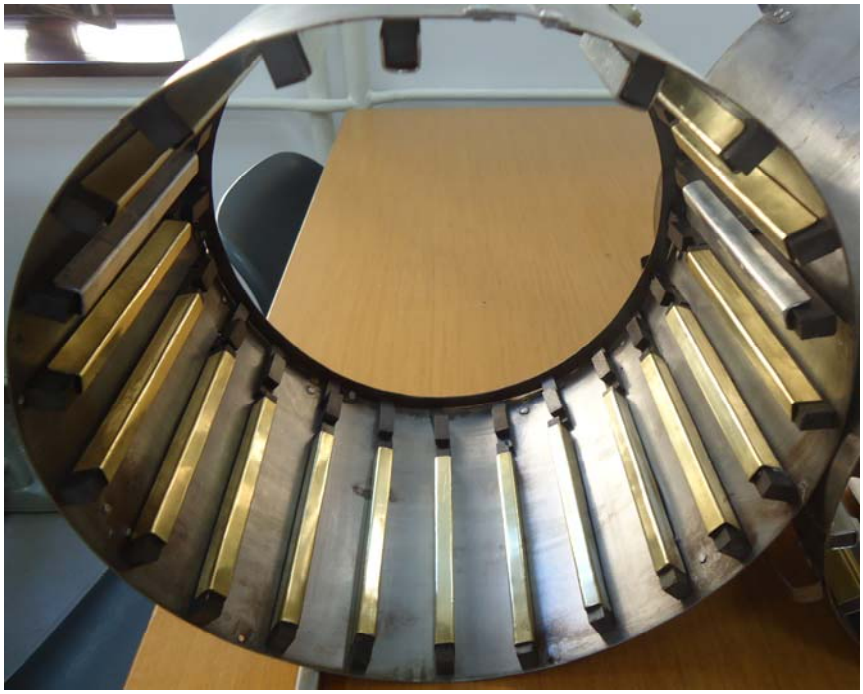

Fig. 5 Photo of the anode of the multi-polar magnetically confined plasma device. The anode is a cylinder made of stainless steel foil (2 mm in thickness). Rows of magnets are mounted on the inner part of the anode.

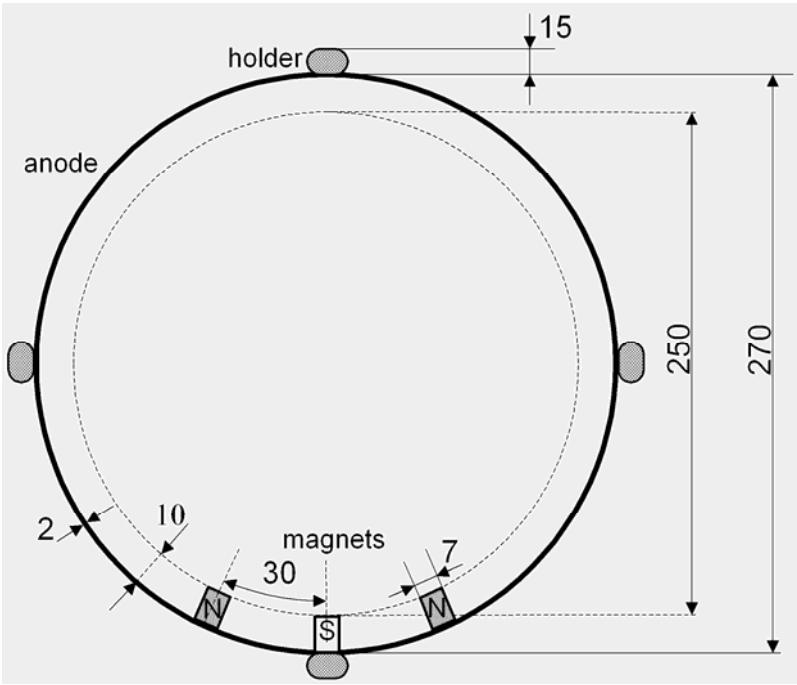

Fig. 6 Technical drawing of the top view of the anode of the multi-polar magnetically confined plasma device.

Note that the inner diameter of the anode with magnets is about 250 mm, this allowing a large volume of magnetically unperturbed plasma. Indeed, the distributions of the radial (B_r) and tangential (B_t) (parallel to the anode wall) of the magnetic field along a radius of the discharge chamber (Fig. 6) shows that the magnetic filed is strong in an anodic sheath with thickness of about 5 cm . This means that probe measurements are not affected by the magnetic filed only if the probes are mounted at a distance larger than 5 cm from the anode. Therefore, the magnetic free region of the multi-polar magnetically confined plasma device is a cylindrical region on the center of the discharge chamber with the diameter of about 150 mm. This means that the probes must be mounted as close possible to the discharge chamber axis (or at a distance smaller than 70 mm from the discharge chamber axis).

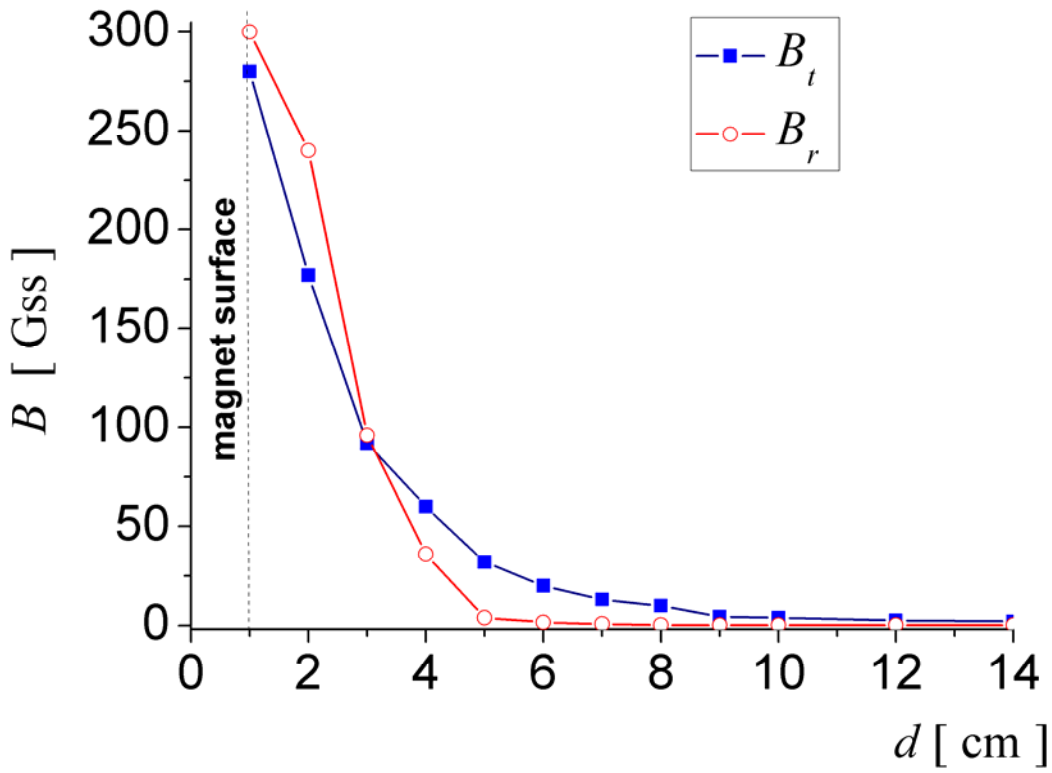

Fig. 7 Distribution of radial (B_r) and tangential (B_t) components of the magnetic field along a radius of the discharge chamber. The radial component was measured along a radius that cross the center of a magnet row, while the tangential component (parallel to the anode wall) was measured along a radius placed between two neighbor rows of magnets, where the parallel component of the magnetic filed is maximum.

The anodes (or the anode) are mounted inside the discharge chamber with the help of six holders that assure a gap distance of about 15 mm between the inner wall of the discharge chamber and the outer surface of the anode. If the anode is insulated electrically from the ground (chamber walls) the holders are made from an electrically insulator material (ceramic). Otherwise, the holders are made from electrically conducting material. Figure 7 shows a photo of the discharge chamber with the anodes mounted inside. In this case there have been used two anodes, one being grounded and the other being insulated.

Fig. 8 Photo of the discharge chamber of the multi-polar magnetically confined plasma device with the anodes mounted inside. The front anode is grounded (the anode holders are made of stainless steel) while the back anode is insulated. The front end of the discharge chamber with the rubber O-ring used for vacuum sealing is clearly visible.

Fig. 9 Photo of one of the cathodes used in the multi-polar magnetically confined plasma device.

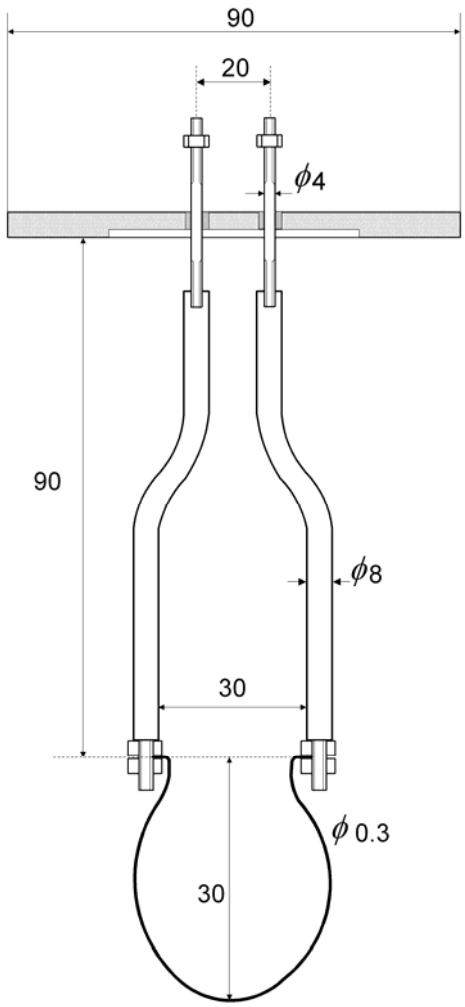

Fig. 10 Technical drawing of the cathode used in the multi-polar magnetically confined plasma device

The two cathodes were mounted on the two upper openings (left and right) of the discharge chamber by the help of two flanges with electrical feed through for direct heating of the filaments. Figure 8 presents a photo of one cathode which shows the flange with the copper electrodes for direct heating of the filament. The filament is made of tungsten wire (0.3 mm in diameter and 9 mm in length) and is mounted on the electrical feeding electrodes with screws. A technical drawing of one cathode where all dimensions are given in mm is represented in Fig 9. The cathodes should be mounted in the openings of the anodes so that the filament is inside the discharge chamber at a distance of few centimeters from the inner side of the anode (as it is seen in the photo presented by Fig 10).

Fig. 11 Photo of the cathode mounted on the discharge chamber of the in the multi-polar magnetically confined plasma device

The flanges are two disks with diameter of 370 mm with various openings used for mounting of the electrical probes and gas feeding. Figure 11 shows the photo of one of the flanges with a Langmuir probe mounted and with an opening used for the gas feeding inlet. Details on the Langmuir probe construction will be given below. On the flange there are mounted circular rows of magnets with alternate polarities (each row has the same polarity and neighbor rows have different polarities) in order to generate the multi-polar magnetic filed used to confine the plasma into the discharge chamber.

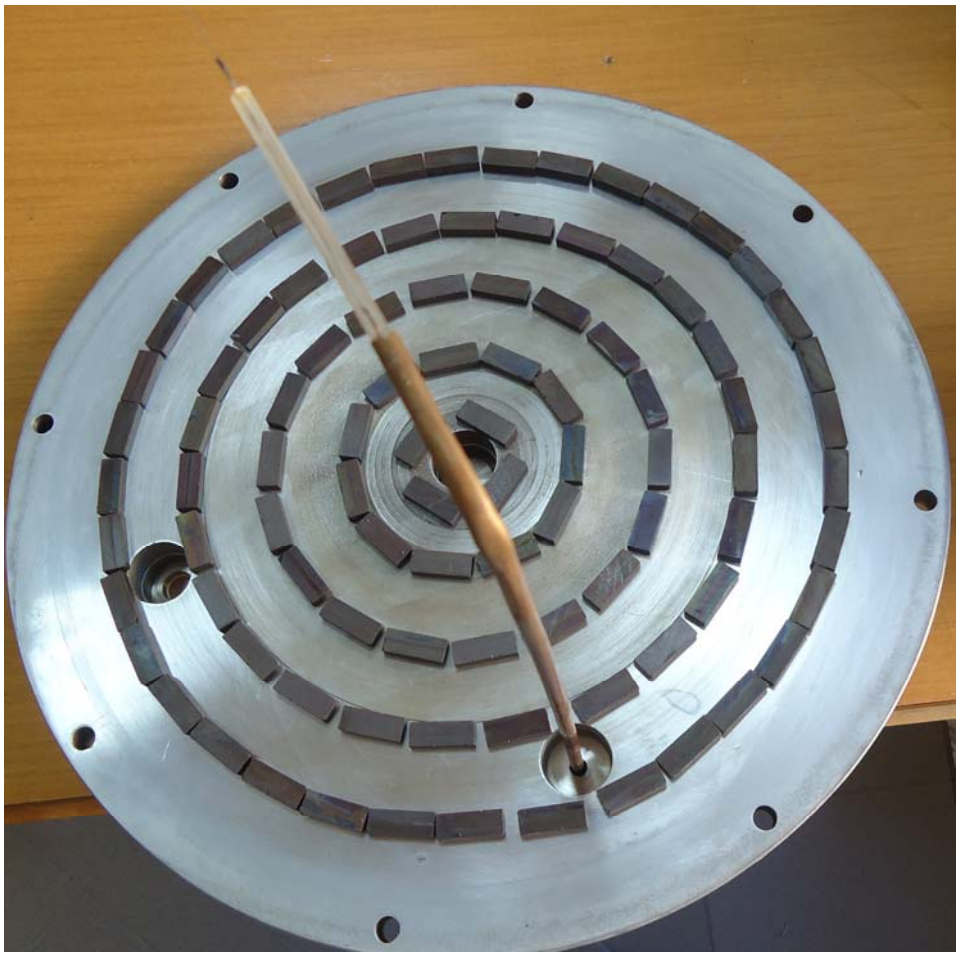

Fig. 12 Photo of a flange used for sealing of one end of the discharge chamber. The flange has one opening on which is mounted a Langmuir probe. Circular rows of magnets are used to generate the multi-polar magnetic field used in plasma confinement.

The discharge chamber is coupled directly to a vacuum pumping system formed by a turbomolecular pump and a dry scroll pump (Turbo-V 301-AG from Agilent Technologies) and mounted on a frame made from iron corner bars. A photo of the plasma machine connected to the vacuum system and mounted on the frame is given in Fig. 12. Figure 13 presents a technical drawing of the frame, vacuum system and discharge chamber (all dimension are given in mm). The vacuum aggregate has a pressure gauge that measure the pressure into the chamber in the range 1000 mbar -10^{-9} mbar. Practically, a minimum pressure of 10^{-5} mbar is achieved in about 15 minutes of pumping (the time can be shorter or longer, function of the vacuum state in the chamber at the moment the pumping started).

The discharge chamber is connected to a gas (argon) supply bottle (visible in the photo in Fig. 12) through a pressure reduction system and a needle valve. The needle valve is used to control the flux of gas that flow through the discharge chamber and thus the gas

pressure. The pressure in the discharge chamber is shown on the screen of the electronic unit of the vacuum aggregate.

To obtain the multi pole magnetically confined plasma, the discharge chamber is vacuumed down to the minimum pressure (the needle valve and the gas feeding system are closed). Then, the gas feeding is open and the pressure into the chamber is adjusted in the range 10^{-3} 10-5 mbar. While the cathode is biased by a discharge power supply (LG 350V 1A from Heisenger) negatively to a potential of about 70 V with the respect of anode, the cathode filament is heated gradually until thermoemission by a direct current from a power supply (LG 32V 6A from Heisenger). To do this, the heating current intensity is increased gradually until a finite discharge current intensity is noticed in the main discharge circuit (see Fig. 1). The discharge current is limited by emission current, so that the discharge current intensity is controlled by the cathode heating current. The heating current intensity is adjusted to have a discharge current intensity ranged between 50 mA and 200 mA. In these conditions the plasma starts inside the chamber, which is noticed by the blue light coming from the visualization window.

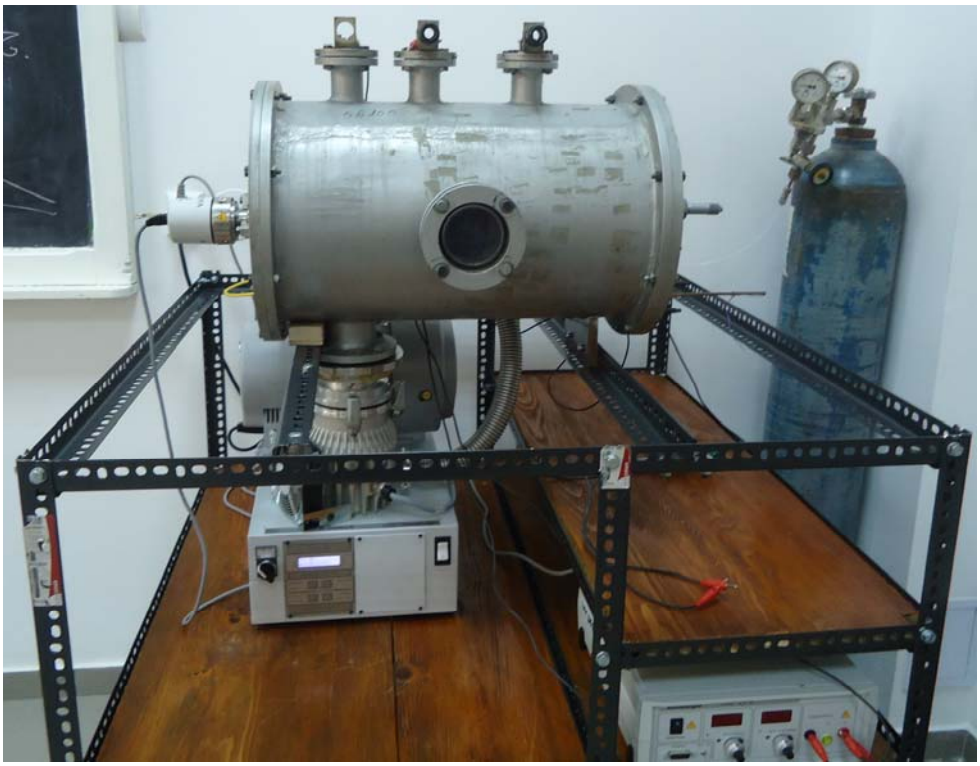

Fig. 13 Photo of the discharge chamber connected to the vacuum aggregate and mounted on the iron frame.

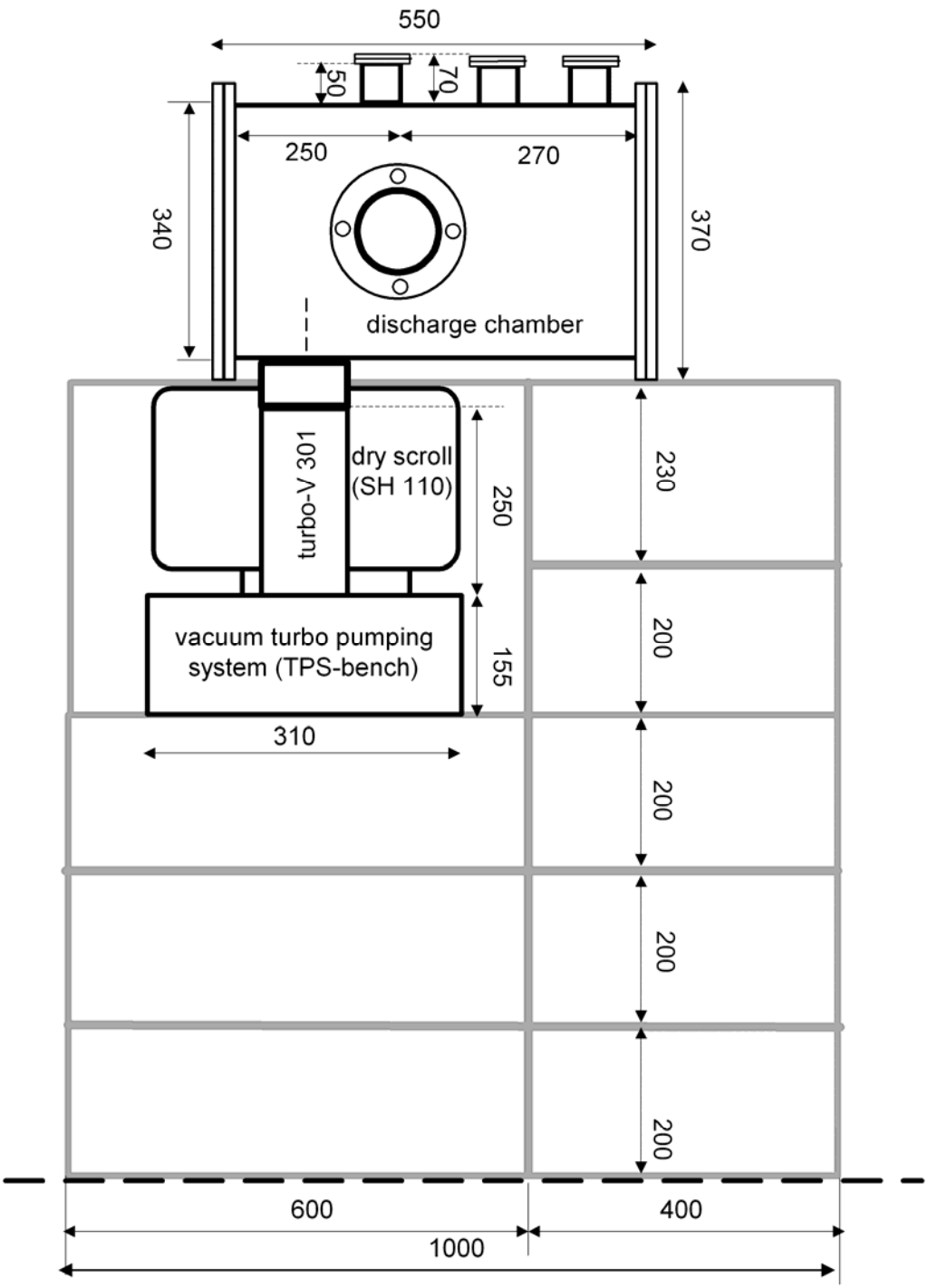

Fig. 14 Technical drawing of the metallic frame used to mount the discharge chamber, the vacuum aggregate, the electrical power supply sources for discharge and cathode heating, and the probe I-V characteristic measuring system.

Figure 14 shows current-voltage characteristics of the electrical discharge that maintain plasma in the multi polar magnetically confined plasma device at three values of cathode emission current. The discharge breaks down at a voltage around 22 V, when the discharge

current rises steeply with the increase of the voltage to values limited by the cathode emission current. The discharge current intensity, the discharge voltage, and the gas pressure are the main discharge parameters that determine the plasma parameters to be measured by the electrical probes, i.e. plasma density, the electron temperature, the plasma potential, and the floating potential. Usually, a stable discharge in argon plasma is operated at a discharge voltage of 70V and discharge current intensity of 100 mA.

Fig. 14. Typical I-V characteristics of electrical discharge in the multi polar magnetically confined plasma device at three values of cathode emission current. The discharge was run in argon at 2×10^{-4} mbar.

2. **Construction of home-made probes (single, double, triple and emissive probe with direct heating)**

Figure 14 presents a photo (a) and a technical drawing (b) of a single cylindrical Langmuir probe made from a tungsten wire (2) with diameter of 0.3 mm and active length (part inserted in plasma) of 7 mm. The tungsten wire (about 50 mm in total length) is connected electrically through a cupper wire (3), which is wrapped around it on a length of about 2 cm, to an electric connector. The tungsten and cupper wires are inserted in a ceramic tube (1) with length of about 100 mm, inner diameter of 0.5 mm and outer diameter of 1.2 mm. The double and triple probes are fabricated on the basis of the same principle [Figures 14 (c) and (d)].

(a)

(b)

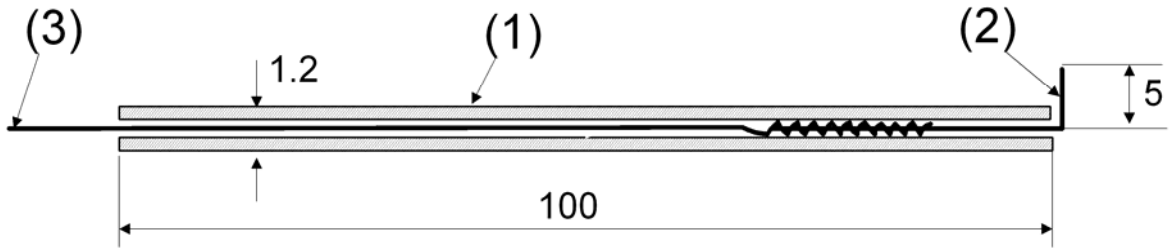

(c)

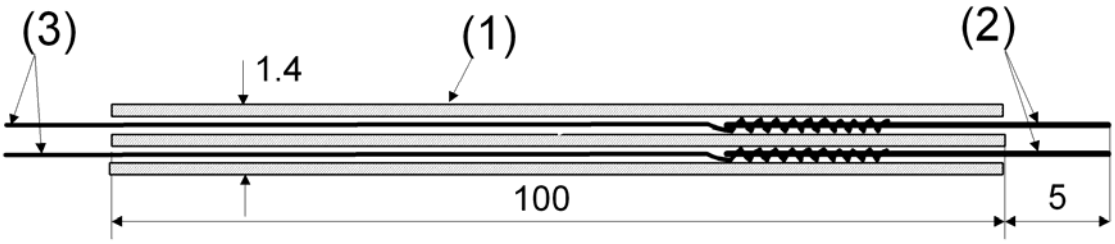

(d)

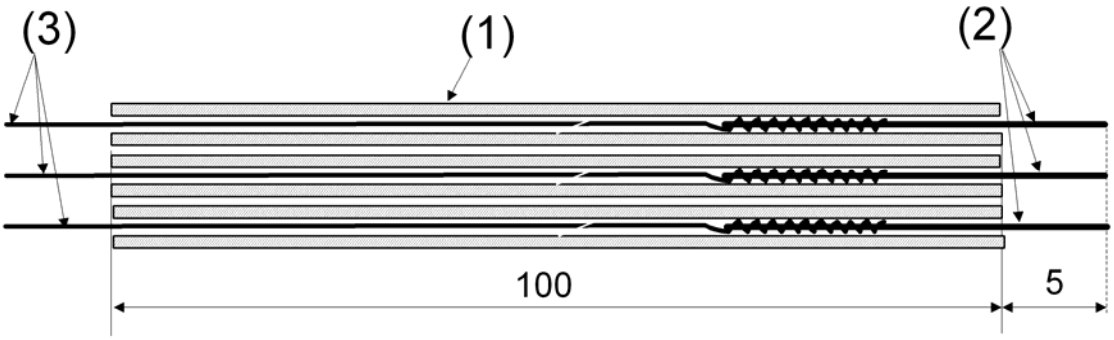

Fig. 15 Photo (a) and technical drawing (b) of a single Langmuir probe. Figures (c) and (d) shows technical drawings of double and triple Langmuir probes, respectively.

The emissive probe has been constructed from a thin tungsten wire (Φ = 0.12 mm) with the length of 4 cm. The wire (2) was bent to make a loop (see Fig. 15) and the ends were inserted in two capillary stainless steel tubes (4). At the free end of capillary tubes were inserted two copper wires (3) for the electrical connection to the heating electrical power supply and biasing electrical power supply. The capillary tubes were pressed to form a firm electrical contact. The loop (2) and the connection wires (3) were inserted into a ceramic tube with two channels.

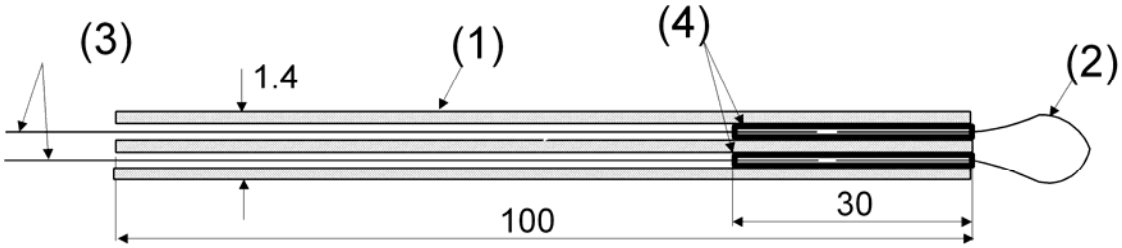

Fig. 15 Technical drawing of an emissive Langmuir probe.

3. Construction of home-made electrostatic analyzer with tree grids.

Figure 17 shows a photo (a) and a technical drawing (b) of the electrostatic analyzer used to determine the energy distribution function of ions in the multipolar magnetically confined plasma. The analyzer is a system of one collector probe (P) with three grids: plasma separating grid (9), which is a floating or a grounded grid that separates the plasma from the analyzer; the electron separation grid (G_2), which is a grid used to reject plasma electrons and biased negatively with respect to the plasma potential at a biased voltage of about -100 V, and secondary electron emission suppression grid (G_1), which is a grid used to reject the electrons emitted by the collector probe (P) by secondary electron emission caused by the energetic positive ions. The whole device is encapsulated in a metal (stainless steel) capsule made from a cylinder (3) and 2 leads (1) and (4). The plasma particles enter into the device through the opening (Φ = 1.2 mm) of a stainless steel diaphragm (2). A stainless steel piece (7) is used to create a distance of about 8 mm between the diaphragm and the plasma separation grid (9), which in this case is grounded as the diaphragm and capsule. The electrical connections to the grids are made through cooper wires which are pressed onto the grids. The plate and grids are mounted on a ceramic piece (5) fixed on the metallic body (3) of the analyzer. The grids are electrically and mechanically separated by small roundels (0.2 mm in thickness, 8mm in inner diameter and 12 mm in outer diameter) made of mica (6). The mesh grid (9) made of stainless steel wires (0.15 mm in diameter) has a spatial constant of 0.25 mm. The mesh grids G_1 and G_2 made of stainless steel wires with diameter of 0.1 mm have a spatial constant of 0.2 mm.

(a)

(b)

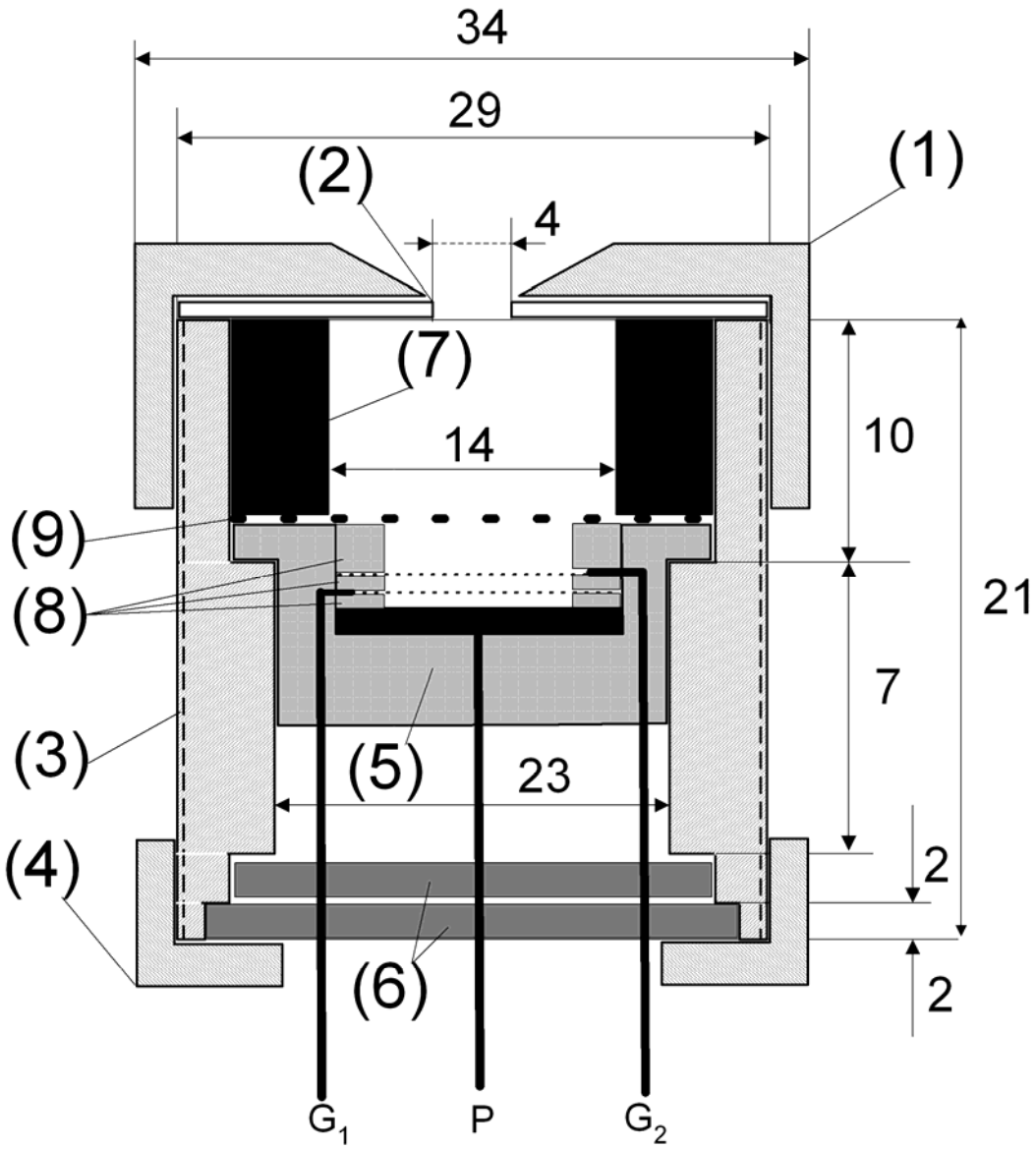

Fig. 14 Photo (a) and technical drawing (b) of a electrostatic analyzer with three grids, plasma separation grid (9), electron separation grid (G_2), and secondary ion emission suppressing grid (G_1). The whole device is encapsulated in a metal (stainless steal) capsule made from a cylinder (3) and 2 leads (1) and (4). The plasma particles enter into the device through the opening (Φ = 1.2 mm) of a diaphragm (2). The diaphragm and the capsule are grounded while the plasma separation grid is floating.